$^{15}N(p,t)^{13}N$ and $^{15}N(p,^3He)^{13}C$ Reactions and the Spectroscopy of Levels in Mass 13*

DONALD G. FLEMING,† JOSEPH CERNY, CREVE C. MAPLES, AND NORMAN K. GLENDENNING
Lawrence Radiation Laboratory and Department of Chemistry, University of California, Berkeley, California
(Received 16 October 1967)

A 43.7-MeV proton beam has been used to induce (p,t) and $(p,^3He)$ reactions on a ^{15}N target. Transitions to mirror final states of ^{13}N and ^{13}C have been investigated over 15 MeV of excitation and several new spin and parity assignments have been made. The distorted-wave Born-approximation (DWBA) predictions of angular distributions for these $^{15}N(p,t)^{13}N$ and $^{15}N(p,^3He)^{13}C$ reactions, using intermediate-coupling wave functions to obtain the two-nucleon structure factors, were generally found to reproduce experiment well; in addition, calculated cross sections for the $^{15}N(p,t)^{13}N$ reaction were in good agreement with the experimental values.

I. INTRODUCTION

IT is the purpose of this paper to discuss the nuclear spectroscopy of the mass-13 nuclei from a comparison of the $^{15}N(p,t)^{13}N$ and $^{15}N(p,^3He)^{13}C$ reactions populating mirror final states. In the past, work at this laboratory has shown that comparisons of (p,t) and $(p,^3He)$ transitions are valuable spectroscopic tools for identifying and characterizing isobaric analog states.[1] However, because analog states were of interest, little work on comparisons of these reactions to other final states, except for that presented in the work of Cerny *et al.*,[2] has been previously reported. For the data discussed herein, such comparisons permit several new spectroscopic assignments to be made.

In the following we attempt to fit both the shapes and the magnitudes of these (p,t) and $(p,^3He)$ transitions with distorted-wave Born approximation (DWBA) calculations,[3,4] thereby testing the mass-13 wave functions of Cohen and Kurath[5] over 15 MeV of excitation. Although many examples of two-nucleon DWBA fits to individual transitions exist in the literature, only recently[6–9] has much attention been paid to the more comprehensive problem of fitting both the shapes and the relative magnitudes of two-nucleon transitions. This report is the first time that such calculations have been extended to cover a wide range of excitation.

II. THEORY

The formulation of the theory of direct two-nucleon transfer reactions by most authors[3,4,10] is essentially equivalent. (An exception is the work of Rook *et al.*,[11] who, in addition to the zero-range interaction employed by others, also use a point-triton approximation.) However, the formulation of Ref. 4 was made with particular emphasis on the role played by the structure of nuclear states in the reaction and will be used throughout this analysis. This theory fully takes into account the coherent effects caused by the spatial and spin correlations between the nucleons in the picked-up pair, which are expressed in the shell model by configuration mixtures.

For details of the theory, the reader is referred to Ref. 4. Here we briefly recapitulate the main ingredients involved in a calculation of two-nucleon transfer reactions. The lowest-order transfer does not entail any rearrangement of nucleons other than those removed from the target and this establishes the *parentage* of the states that can be excited. Further, because the nucleons are transferred to or from a light nuclide having simple and presumably known[12] *spatial and spin correlations*, a nuclear state is excited only to the extent that these pair correlations are present.[4] This information is conveniently incorporated into a calculation of the cross section through the function which describes the center-of-mass motion of the transferred pair, when they are appropriately correlated and when the nuclear state has

* Work performed under the auspices of the U. S. Atomic Energy Commission.
† Now at the Nuclear Structure Laboratory, University of Rochester, Rochester, N. Y.
[1] J. Cerny and R. H. Pehl, Phys. Rev. Letters **12**, 619 (1964); J. Cerny, R. H. Pehl, and G. T. Garvey, Phys. Letters **12**, 234 (1964); G. T. Garvey, J. Cerny, and R. H. Pehl, Phys. Rev. Letters **12**, 726 (1964); C. Detraz, J. Cerny, and R. H. Pehl, *ibid.* **14**, 708 (1965); J. Cerny, R. H. Pehl, G. Butler, D. G. Fleming, C. Maples, and C. Detraz, Phys. Letters **20**, 35 (1966).
[2] J. Cerny, C. Detraz, and R. H. Pehl, Phys. Rev. **152**, 950 (1966).
[3] N. K. Glendenning, Ann. Rev. Nucl. Sci. **13**, 191 (1963).
[4] N. K. Glendenning, Phys. Rev. **137**, B102 (1965).
[5] S. Cohen and D. Kurath, Nucl. Phys. **73**, 1 (1965); D. Kurath (private communication).
[6] J. J. Wesolowski, L. F. Hansen, J. G. Vidal, and M. L. Stelts, Phys. Rev. **148**, 1063 (1966); J. Vervier, Phys. Letters **22**, 82 (1966); **24B**, 603 (1967); R. K. Cole, R. Dittman, H. S. Sandhu, and C. N. Waddell, Nucl. Phys. **A91**, 665 (1967).
[7] R. A. Broglia and C. Riedel, Nucl. Phys. **A92**, 145 (1967); **A93**, 241 (1967).
[8] N. F. Mangelson and B. G. Harvey, Lawrence Radiation Laboratory Annual Report No. UCRL-17299, 1966, p. 97 (unpublished); N. F. Mangelson (private communication).
[9] N. K. Glendenning, Phys. Rev. **156**, 1344 (1967).
[10] C. L. Lin and S. Yoshida, Progr. Theoret. Phys. (Kyoto) **32**, 885 (1964); E. M. Henley and D. V. L. Yu, Phys. Rev. **133**, B1445 (1964); B. Bayman, Argonne National Laboratory Report No. ANL-6878, 1964, p. 335 (unpublished); A. Y. Abul-Magd and M. El. Nadi, Nucl. Phys. **77**, 182 (1966); C. Lin, Progr. Theoret. Phys. (Kyoto) **36**, 251 (1966).
[11] J. R. Rook and D. Mitra, Nucl. Phys. **51**, 96 (1964); J. R. Rook and V. S. Mathur, *ibid.* **A91**, 305 (1967).
[12] We assume pure relative-s-state motions, which is known to be at least 94% good for the triton g.s. [J. M. Blatt, G. H. Derrick, and J. N. Lyness, Phys. Rev. Letters **8**, 323 (1962); R. Pascual, *ibid.* **19**, 221 (1965); B. F. Gibson, Phys. Rev. **139**, 1153 (1965)].

the required parentage. Then, in the DWBA treatment, a calculation of the cross section involves evaluation of the usual type of integrals[3,4] involved in all direct reactions, with the above-described center-of-mass wave function entering as the "form factor."

Since most nuclear-structure calculations employ harmonic-oscillator functions (in any case, all single-particle wave functions can be expanded in terms of them), the projected center-of-mass wave function for the two-nucleon transfer reaction can be written as

$$\tilde{U}_L(R)=\sum_N G_{NLSJT}U_{NL}(2\nu R^2),$$

where U_{NL} is a harmonic-oscillator function and $\nu=m\omega/\hbar$ is a constant corresponding to the particular single-particle motions involved. Because of the poor asymptotic behavior of the oscillator functions, $\tilde{U}_L(R)$ is matched (at the nuclear surface) to the appropriate Hankel function with asymptotic behavior corresponding to the separation energy of the pair.

The structure amplitudes G_{NLSJT} are calculated from the wave functions used to describe the initial and final nuclear states. They carry all the nuclear-structure information relevant to the reaction and their explicit form was given previously.[4] Generally, they involve a sum over several configurations of the pair since this is the way in which correlations are expressed in the shell model.

One of the factors involved in the calculation of the structure amplitude G_{NLSJT} is the parentage factor $\beta[(j_1j_2)_J]$ that measure the degree to which the state of the nucleus $(A+2)$ has as its parent the nucleus (A), with the transferred pair in the state $(j_1j_2)_J$. Using the general definition of Ref. 4, the parentage factors for several types of configurations[5] excited in the ^{15}N$(p,t)^{13}$N and ^{15}N$(p,^3$He$)^{13}$C reactions[13] are now given (a neutron-proton formalism is used).

The target wave function has spin j and is written as

$$|\psi_T\rangle=|(j_a{}^{n_a})_0(j_b{}^{n_b})_0,j;j\rangle.$$

(1) For a pair of like nucleons added or taken out of a given shell—say j_b—where n_b is even, the final-state wave function has the form

$$|\psi_F\rangle=|(j_a{}^{n_a})_0,(j_b{}^{n_b-2})_J,j;J_f\rangle.$$

The parentage factor relating initial- and final-state configurations for a particular total-angular-momentum transfer J and a particular final-state spin J_f is

$$\beta[(j_b)^2_J]=\left(\frac{n_b(n_b-1)}{2}\right)^{1/2}((j_b{}^{n_b-2})_{\nu J}(j_b{}^2)_J;0|\}(j_b{}^{n_b})_0)\times\left(\frac{2J_f+1}{(2J+1)(2j+1)}\right)^{1/2}.$$

Explicit expressions for the two-nucleon coefficients of fractional parentage ($|\}$) may be found in Ref. 4 or in the work of Schwartz and de-Shalit.[14]

(2) For a pair of nucleons transferred across shells or a pair of nonidentical nucleons (a neutron-proton pair) transferred within the same shell, the final-state wave function has the form

$$|\psi_F\rangle=|[(j_a{}^{n_a-1})_{j_a}(j_b{}^{n_b-1})_{j_b}]_J,j;J_f\rangle,$$

where the square bracket denotes vector coupling and n_a and n_b are even. The parentage factor relating this configuration to the initial state by the total-angular-momentum transfer J is given by

$$\beta[(j_a,j_b)]_J=(n_an_b)^{1/2}\left(\frac{2J_f+1}{(2j_a+1)(2j_b+1)(2j+1)}\right)^{1/2}.$$

The DWBA calculation[4] involves use of these parentage factors in LS coupling and this is achieved by the appropriate jj-LS transformation coefficient. The calculation for states of mixed configuration[5] involves the appropriate linear combination of the above β's. Explicit derivations of these expressions are given by Fleming.[15]

III. EXPERIMENTAL

These reactions were induced by a 43.7-MeV proton beam from the Berkeley spiral-ridge cyclotron. The physical layout of the cyclotron and target area, together with the over-all beam optics, is illustrated in Fig. 1. In the radial plane, the first set of quadrupole magnets (Quad. 1) creates an image of the virtual source just prior to the entrance of the switching magnet. The beam is then deflected 38° by the switching magnet through a second set of quadrupole magnets (Quad. 3) which produces a radial focus at the analyzing slit. For our experiments, this slit consisted of two vertical tantalum plates 125 mils thick and normally set 60 mils apart. In the vertical plane, only one focus is required prior to the scattering chamber. This occurs at the exit of the switching magnet. Beyond the analyzing slit, two quadrupole lens doublets (Quad. 21, Quad. 22) were required to bring the beam to a radial and vertical focus at the center of a 20-in.-diam scatter chamber. Typical beam-spot sizes at this point were 80 mils wide×100 mils high, with beam intensities varying between 0.05 and 1.0 μA, as required. The beam current was measured in a Faraday cup with an integrating electrometer.

Reaction events were measured in two separate counter telescopes, each consisting of a 5.5-mil phosphorus-diffused silicon ΔE detector and a 120-mil lithium-drift silicon E detector, backed by a 20-mil lithium-drift silicon detector. This last counter served

[13] These parentage factors (with the possible exception of a phase change) are generally true for any two-nucleon transfer reaction on an odd-mass target which involves a single (extracore) nucleon.

[14] C. Schwartz and A. de-Shalit, Phys. Rev. 94, 1257 (1954).

[15] D. G. Fleming, Ph.D. thesis, University of California Lawrence Radiation Laboratory Report No. UCRL-17790, 1967 (unpublished).

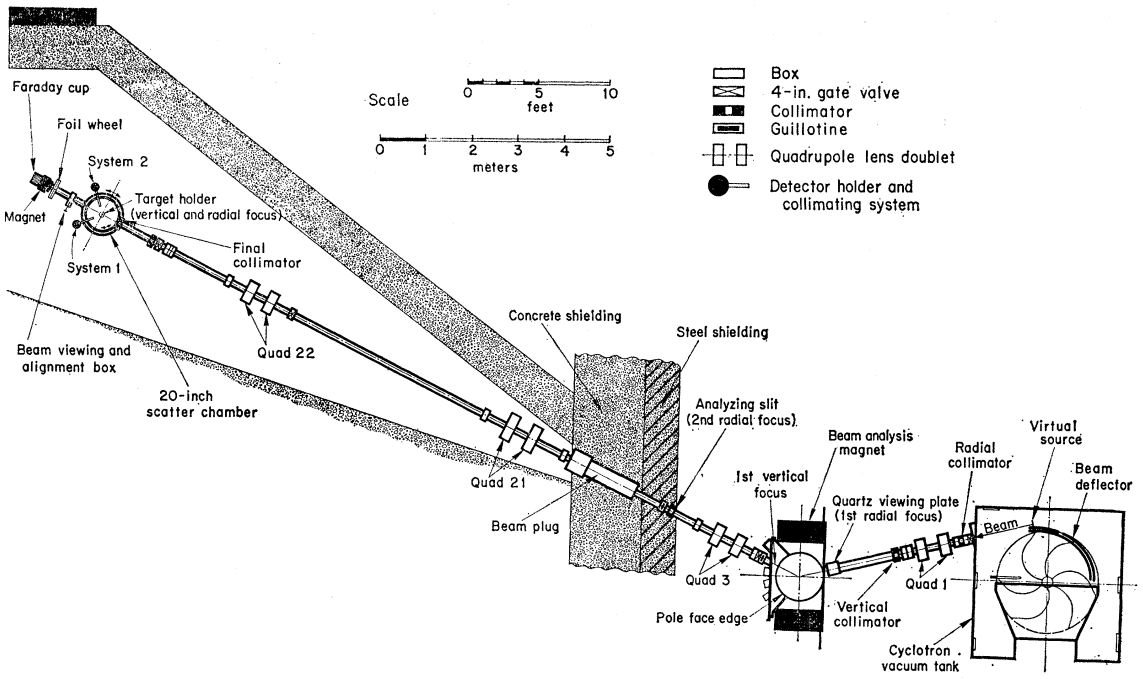

FIG. 1. Cyclotron layout and beam optics.

to eliminate signals from long-range events which passed through the first detectors. The target was 99% pure $^{15}N_2$ gas and was contained in a 3-in.-diam gas cell which was filled externally. A 315° gas target window was covered with 0.1-mil Haver foil[16] which easily withstood pressures of 30 cm of mercury. The target pressure and beam energy were constantly monitored by a 120-mil lithium-drifted silicon detector fixed at 27.5° to the beam.

A block diagram of the electronics is shown in Fig. 2. Signals from the three detectors (ΔE,E,E_{rej}) were first sent to charge-sensitive preamplifiers, which then fed the main amplifiers in the circuit. ΔE and E signals from these amplifiers were then fed to a Goulding-

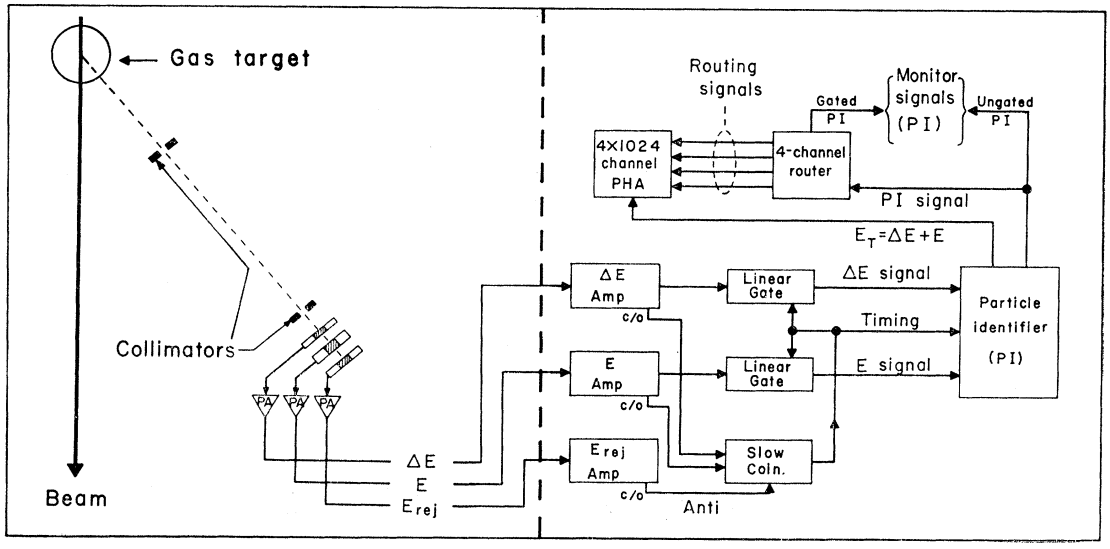

FIG. 2. A counter assembly and a block diagram of the electronics used in these experiments.

[16] Hamilton Watch Co., Lancaster, Pa.

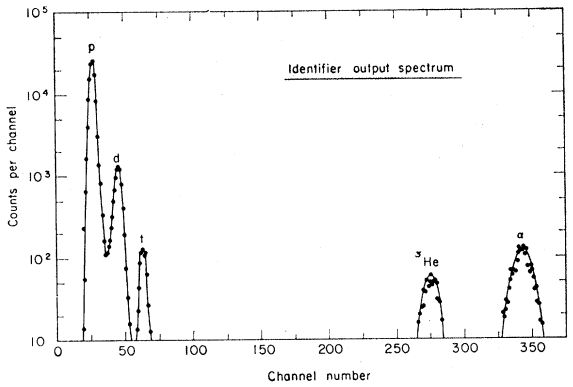

FIG. 3. A typical particle-identifier spectrum.

Landis particle identifier.[17] This unit operates on the empirical relation $R=aE^{1.73}$, where R is the range of the particle, E is its total energy, and a is a constant characteristic of the particle type. A particle identifier spectrum is shown in Fig. 3. Particle identifier signals were selectively gated in a four-channel router so that valid triton, helium-3 (and α particle) events could be recorded in the appropriate channel of a Nuclear Data analyzer or in an on-line PDP-5 computer, both operating in a 4×1024-channel mode. Since it was not always possible to completely separate deuterons and tritons with this relatively thin ΔE detector, a safety group was observed in which any leak-through tritons were collected. Energy resolutions [full width at half-maximum (FWHM)] of 150 and 180 keV were obtained for tritons and helium-3, respectively.

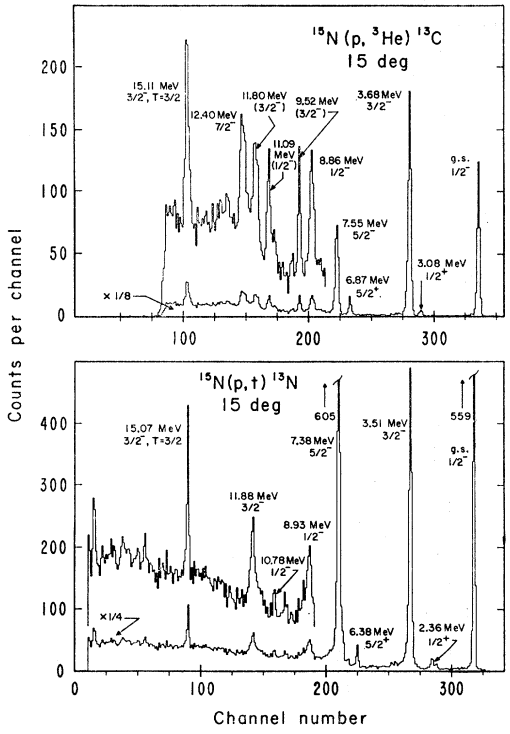

FIG. 4. Energy spectra for the $^{15}N(p,t)^{13}N$ and $^{15}N(p,^3He)^{13}C$ reactions. The spectra have been adjusted to match channels for the $\frac{5}{2}^-$ transitions, showing a slight nonlinearity in the triton spectrum at the higher energies.

[17] F. S. Goulding, D. A. Landis, J. Cerny, and R. H. Pehl, Nucl. Instr. Methods **31**, 1 (1964).

TABLE I. Integrated cross sections of the ^{13}N levels observed in the $^{15}N(p,t)^{13}N$ reaction and comparison of these states with those previously reported.

$^{15}N(p,t)^{13}N$			Previously reported[b]	
J^π	Excitation[a] (MeV±keV)	$\sigma_T(\mu b)$ (10°–90°, c.m.)	J^π	Excitation (MeV±keV)
$\frac{1}{2}^-$	*0.0 ±25	941±20	$\frac{1}{2}^-$	0.0
$\frac{1}{2}^+$	2.36±30	Very weak	$\frac{1}{2}^+$	2.366±2
$\frac{3}{2}^-$	*3.51±30	652±25	$\frac{3}{2}^-$	3.510±2
$\frac{5}{2}^+$	6.38±30	63±7	$\frac{5}{2}^+$	6.382
$\frac{5}{2}^-$	*7.38±20	1271±44	$\frac{5}{2}^-$	7.385±8
$\frac{1}{2}^-$	8.93±50	130±16	$\frac{1}{2}^-$	8.90
	Not observed		$\frac{3}{2}^-$	9.48
$\frac{1}{2}^-$	10.78±60	17.6±4	Not reported	
$\frac{3}{2}^-$	11.88±40	93±9	$\frac{3}{2}^-$[c]	11.85
$\frac{3}{2}^-$	*15.07±20	115±11	$\frac{3}{2}^-$	15.068±8
$[T=\frac{3}{2}]$			$[T=\frac{3}{2}]$	

[a] Levels marked with an asterisk were considered known in the energy analysis.
[b] Reference 18.
[c] Spin and parity assigned in Refs. 19 and 20.

IV. RESULTS

Figure 4 presents energy spectra of the $^{15}N(p,t)^{13}N$ and $^{15}N(p,^3He)^{13}C$ reactions taken at 15° in the laboratory. The excitations shown were obtained in this experiment and for the most part agree with previous values,[18] as shown in Tables I and II. Those levels

TABLE II. Integrated cross sections of the ^{13}C levels observed in the $^{15}N(p,^3He)^{13}C$ reaction and comparison of these states with those previously reported.

$^{15}N(p,^3He)^{13}C$			Previously reported[b]	
J^π	Excitation[a] (MeV±keV)	$\sigma_T(\mu b)$ (10°–90°, c.m.)	J^π	Excitation (MeV)
$\frac{1}{2}^-$	*0.0 ±15	308±18	$\frac{1}{2}^-$	0.0
$\frac{1}{2}^+$	3.08±20	Very weak	$\frac{1}{2}^+$	3.086±3
$\frac{3}{2}^-$	*3.68±10	573±20	$\frac{3}{2}^-$	3.681±3
$\frac{5}{2}^+$	*6.87±15	42±5	$\frac{5}{2}^+$	6.866±7
$\frac{5}{2}^-$	7.55±20	270±18		7.55 ±15
$\frac{1}{2}^-$	8.86±60	61±9	$\frac{1}{2}^-$	8.86 ±20
$(\frac{3}{2}^-)$	9.52±30	71±12		9.503±15
$(\frac{1}{2}^-)$	11.09±50	52±7		11.078±20
$(\frac{3}{2}^-)$	11.80±30	137±14		11.721±30
$\frac{7}{2}^-$	12.40±50	100±10	$(\frac{1}{2}^-)$	12.45
$\frac{3}{2}^-$	*15.11±20	[c]88±7	$\frac{3}{2}^-$	15.113±5
$[T=\frac{3}{2}]$			$[T=\frac{3}{2}]$	

[a] Levels marked with an asterisk were considered known in the energy analysis.
[b] Reference 18.
[c] Integrated to 65°, c.m.

[18] F. A. Selove, *Energy Levels of Light Nuclei* (National Academy of Science—National Research Council, Washington, D. C., 1962); also (private communication).

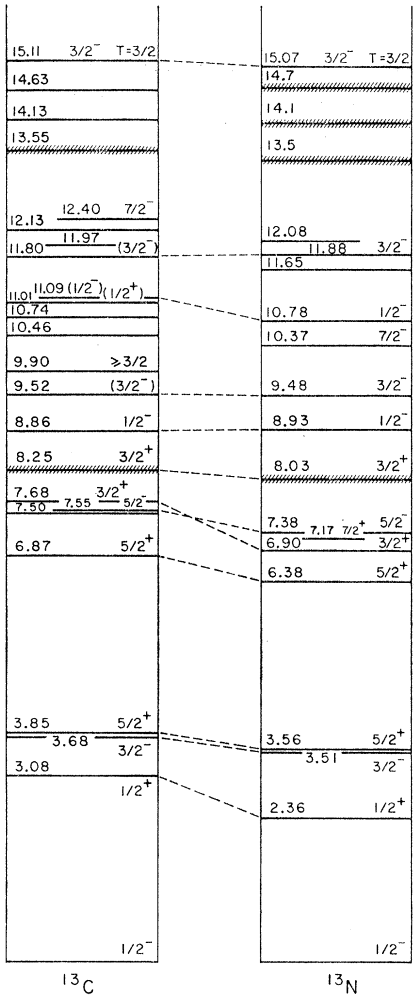

FIG. 5. Energy-level diagram for ^{13}N and ^{13}C.

marked with an asterisk in these tables were used to determine the energy scale and their associated errors (in keV) reflect the over-all uncertainties involved in the analysis. In addition, spin and parity assignments

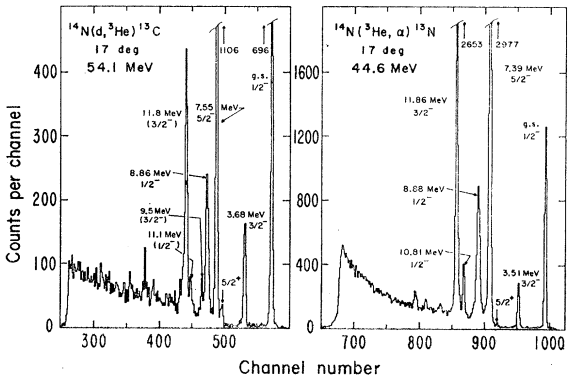

FIG. 6. Energy spectra of the ^{14}N(d,^{3}He)^{13}C and ^{14}N(^{3}He,α)^{13}N reactions.

are presented in these tables, and these will be fully explained later in the text. An energy-level diagram for ^{13}C and ^{13}N is presented in Fig. 5. The data in Fig. 4 show that the reaction is very selective, strongly populating only the negative-parity states in the mass-13 nuclei. This is expected on the basis of a direct pickup of two nucleons from a $(1p)^{11}$ configuration, which is assumed for the ground state of ^{15}N. However, some positive-parity levels are excited relatively strongly and their presence in the spectra will also be discussed. Figure 6 presents energy spectra for the ^{14}N(^{3}He,α)^{13}N and ^{14}N(d,^{3}He)^{13}C reactions[19] taken at a laboratory angle of 17°, which will be used to support some of the later discussion. Similar data on single-nucleon transfer reactions populating states in ^{13}N have been obtained in recent ^{14}N(p,d)^{13}N experiments.[20]

Angular distributions for levels excited in the ^{15}N(p,t)^{13}N and ^{15}N(p,^{3}He)^{13}C reactions are shown in Figs. 7–12; the statistical errors are contained within the points unless explicitly indicated. The total integrated cross sections for these reactions are presented

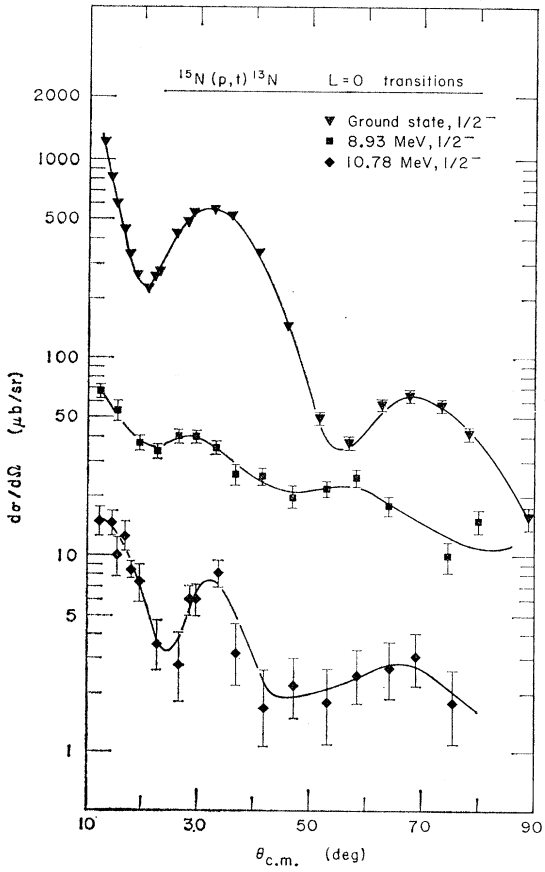

FIG. 7. ^{15}N(p,t)^{13}N L=0 angular distributions. The curves are drawn through the data and have no theoretical significance.

[19] G. Ball and J. Cerny (to be published).
[20] D. Bachelier, M. Bernas, I. Brissaud, P. Radvanyi, and M. Roy, Nucl. Phys. **88**, 307 (1966); R. L. Kozub, L. A. Kull, and E. Kashy, *ibid.* **A99**, 540 (1967).

in Tables I and II; the absolute errors on the large transitions are expected to be $\leq 10\%$. Representative relative errors for all states are given in these tables. Of later interest will be Figs. 13 and 14, which present (p,t) $L=0$ and $L=2$ angular distributions obtained on a variety of light nuclei. These are remarkably similar in shape, considering the range of particle energies involved. Hintz and co-workers[21] have observed similar effects in (p,t) reactions on heavier nuclei.

V. DISCUSSION

We wish to analyze the negative-parity levels excited in the $^{15}N(p,t)^{13}N$ and $^{15}N(p,^3He)^{13}C$ reactions. The energy levels observed are compared with those predicted by intermediate coupling theories and the experimental angular distributions are compared with the two-nucleon transfer theory of Ref. 4. Later, the performance of this theory in predicting relative cross sections for these transitions is noted. However, prior

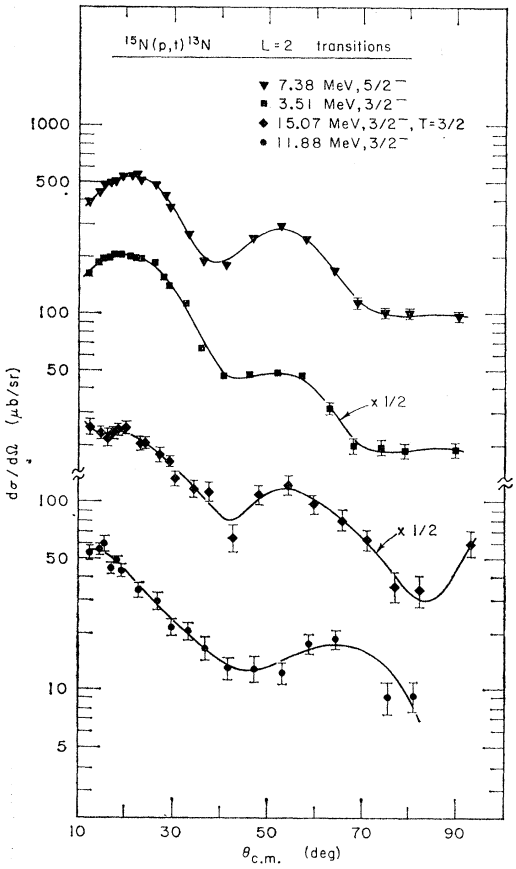

FIG. 8. $^{15}N(p,t)^{13}N$ $L=2$ angular distributions. The curves have no theoretical significance.

[21] G. Bassani, N. M. Hintz, C. D. Kavaloski, J. R. Maxwell, and G. M. Reynolds, Phys. Rev. **139**, B830 (1965); J. R. Maxwell, G. M. Reynolds, and N. M. Hintz, *ibid.* **151**, 1000 (1966); Phys. Letters **22**, 454 (1966); G. M. Reynolds, J. R. Maxwell, and N. M. Hintz, Phys. Rev. **153**, 1283 (1967).

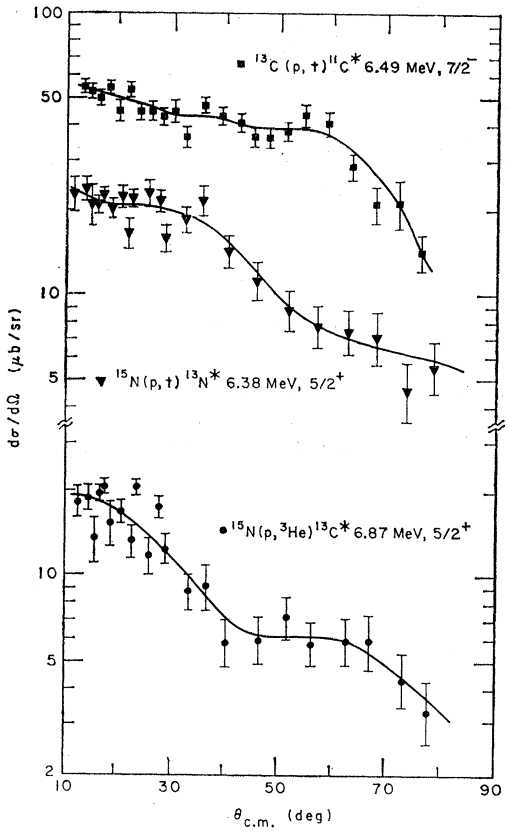

FIG. 9. Angular distributions for the $^{13}C(p,t)^{11}C$ 6.49-MeV, the $^{15}N(p,t)^{13}N$ 6.38-MeV, and the $^{15}N(p,^3He)^{13}C$ 6.87-MeV transitions. The curves have no theoretical significance.

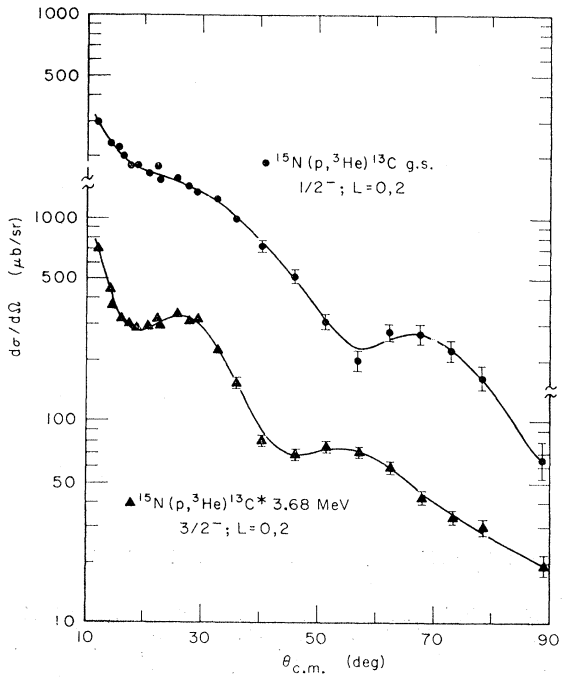

FIG. 10. The $L=0$, 2 angular distributions of the $^{15}N(p,^3He)^{13}C$ g.s. and 3.68-MeV transitions. The curves have no theoretical significance.

to these analyses the optical-model parameters used in this study require discussion.

Since appropriate elastic-scattering data were not available in either the entrance or the exit channel, the optical-model parameters were obtained from an examination of the "best-fit" parameters available in the literature. There are only a few reports of about 40-MeV proton scattering on light nuclei,[22,23] and, unlike what is available in our code, most of these fits[22] have employed a spin-orbit term in the optical potential. However, we are able to employ a real well depth which is consistent with the values given in Refs. 22 and 23, though the absorptive potential had to be increased considerably. The proton potential that proved to give the best over-all fit to the data was interpolated from a graph of optical-model parameters versus energy, given by Bjorklund.[24]

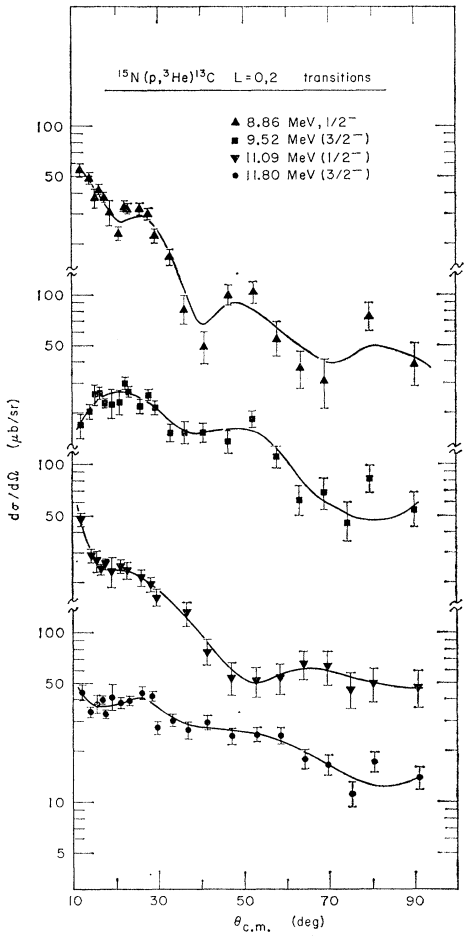

FIG. 11. ^{15}N(p,^{3}He)^{13}C $L=0$, $L=2$ angular distributions. The curves have no theoretical significance.

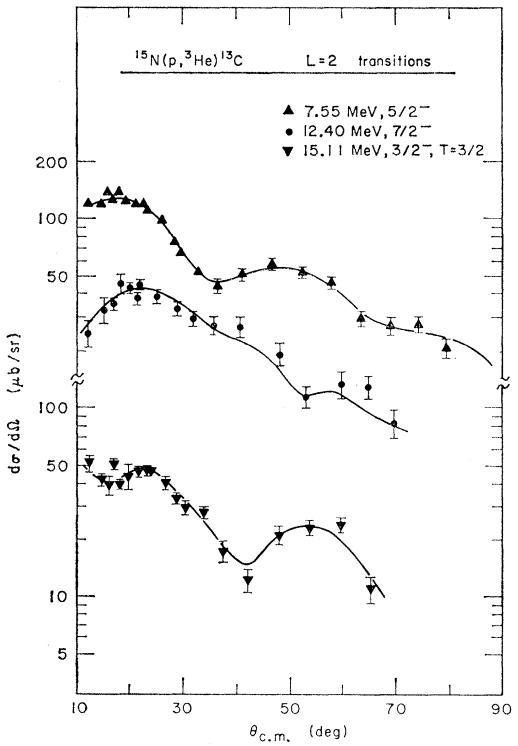

FIG. 12. ^{15}N(p,^{3}He)^{13}C $L=2$ angular distributions. The curves have no theoretical significance.

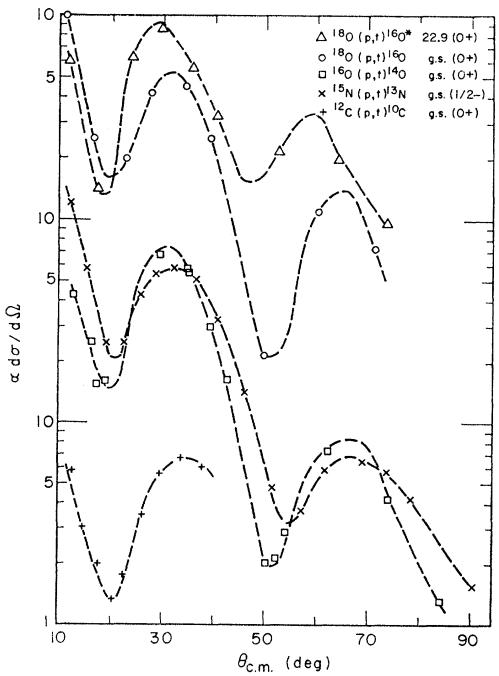

FIG. 13. "Standard" (p,t) $L=0$ angular distributions obtained on a variety of light nuclei.

[22] M. P. Fricke and G. R. Satchler, Phys. Rev. **139**, B567 (1965); E. T. Boschitz, M. Chabre, H. E. Conzett, and R. J. Slobodrian, Lawrence Radiation Laboratory Annual Report No. UCRL-16580, 1965, p. 118 (unpublished); J. A. Fannan, E. J. Burge, D. A. Smith, and N. K. Ganguly, Nucl. Phys. **A97**, 263 (1967).

[23] A. E. Glassgold and P. J. Kellog, Phys. Rev. **109**, 1291 (1958).

[24] F. Bjorklund, in Proceedings of the International Conference on Nuclear Optical Model, Florida State University, 1959, p. 1 (unpublished).

TABLE III. Optical-model potentials.[a] $-U(r)=Vf(r)+iWf(r)-4aiW_Df'(r)-V_c(r)$.

Channel	V (MeV)	W (MeV)	W_D (MeV)	a_V (F)	a_W (F)	a_{W_D} (F)	r_V (F)	r_{W,W_D} (F)	r_c (F)
$^{15}N+p$ (A)	34.0		22.0	0.65		0.50	1.25	1.25	1.30
$^{13}N+t$ (X)	153.0		16.0	0.65		0.54	1.25	1.25	1.30
$^{13}N+t$ (Y)	63.4	62.8		0.58	0.58		1.61	1.61	1.30
$^{13}N+t$ (Z)	220.0	23.8		0.53	0.99		1.22	1.80	1.30

[a] *Note added in proof.* The geometrical parameters (r,a) for the proton optical potentials listed in this and the associated paper [Phys. Rev. **165**, 1153 (1968)] that were actually used are smaller than those listed in the tables by the ratio or the heavy nuclei involved. We are indebted to Dr. John Hardy for discovering a discrepancy between our program and another.

The choice of an exit-channel potential—in the absence of elastic-scattering data—is perhaps subject to the most uncertainty. In accord with the hypothesis that in a reaction involving complex particles one should consider the interaction of each nucleon with the scattering center,[25,26] we have used triton and helium-3 optical-model parameters corresponding to a sum of single-nucleon potentials. These were obtained from searching the literature for the appropriate low-energy (about 10 MeV) nucleon scattering data on light nuclei.[27] Parameters obtained in this way are similar to those found from helium-3 optical-model fits on light nuclei[28] in the energy region of our experiment (about 25 MeV), although this reference generally employed larger radii for the imaginary well. (There are no optical-model parameters available for triton scattering on light nuclei at these energies.) The best "summed" potential was determined from the $^{15}N(p,t)^{13}N$ data alone since only a single L transfer was allowed in these transitions and this potential is presented in Table III (potential X) along with the proton potential[24] mentioned above (potential A). The exit-channel parameters were taken to be the same for both tritons and helium-3 and are labeled just by the triton channel in Table III. Earlier work in fitting helium-3 elastic-scattering data on light nuclei[29] employed a "shallow" potential for the real well depth and an average of the parameters given in Ref. 29 is shown in Table III (potential Y). In addition, Table III contains a potential found[8] from 30-MeV helium-3 scattering on ^{12}C (potential Z). The combination that produced the best over-all results—over 15 MeV of excitation—was AX. Although the proton potential was relatively insensitive to the choice of volume or surface (derivative Saxon-Wood) absorption, the triton potential in the AX combination gave better over-all fits to the data with surface absorption.

DWBA fits to the data are compared in Figs. 15 and 16 for the $^{15}N(p,t)^{13}N$ ground-state ($L=0$) and $^{15}N(p,t)^{13}N$ 7.38-MeV ($L=2$) transitions, respectively, utilizing the potentials AX, AY, and AZ of Table III. The fits have all been arbitrarily normalized to the data, at 32° for the ground-state transition (Fig. 15) and at 20° for the 7.38-MeV transition (Fig. 16). These are the two strongest states in the spectrum, so that they should be good tests for the correctness of the optical-model wave functions. The ground-state transition ($L=0$) is best fit with potential AZ while the 7.38-MeV transition ($L=2$) is best fit with potential AX. However, AX generally fits the other transitions in the (p,t) data better than AZ does. For both transitions, the "shallow" potential AY gives a relatively poor fit to the data. All of the (p,t) and $(p,^3He)$ fits discussed in the following have been calculated with the potential AX. Attempts to improve the DWBA fits to excited states through introducing an energy dependence in the triton potential by reducing the real well

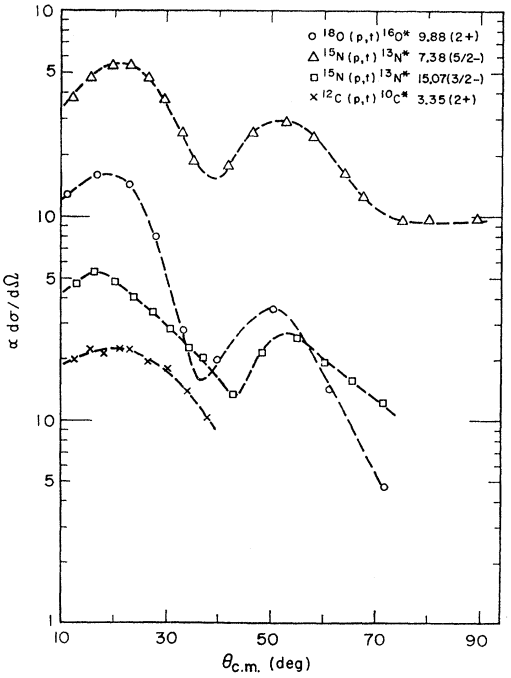

FIG. 14. "Standard" (p,t) $L=2$ angular distributions obtained on a variety of light nuclei.

[25] R. N. Glover and A. D. W. Jones, Phys. Letters **16**, 69 (1965); J. R. Rook, Nucl. Phys. **61**, 219 (1965); K. R. Greider and W. R. Dodd, Phys. Rev. **146**, 671 (1966).
[26] R. N. Glover and A. D. W. Jones, Nucl. Phys. **81**, 277 (1966).
[27] W. W. Daehnick, Phys. Rev. **135**, B1168 (1964); B. Johansson, Nucl. Phys. **67**, 285 (1965); J. Stevens, H. F. Lutz, and S. F. Eccles, *ibid.* **76**, 129 (1966); A. J. Frasca, R. W. Finlay, R. O. Koshel, and R. L. Cassola, Phys. Rev. **144**, 854 (1966).
[28] J. C. Hiebert, E. Newman, and R. H. Bassel, Phys. Rev. **154**, 898 (1967).
[29] P. E. Hodgson, in *Proceedings of the Rutherford Jubilee International Conference, Manchester, England, 1961*, edited by J. B. Birks (Heywood and Company, Ltd., London, 1962), p. 407; H. M. Sen Gupta, J. Rotblatt, P. E. Hodgson, and J. B. A. England, Nucl. Phys. **38**, 361 (1962).

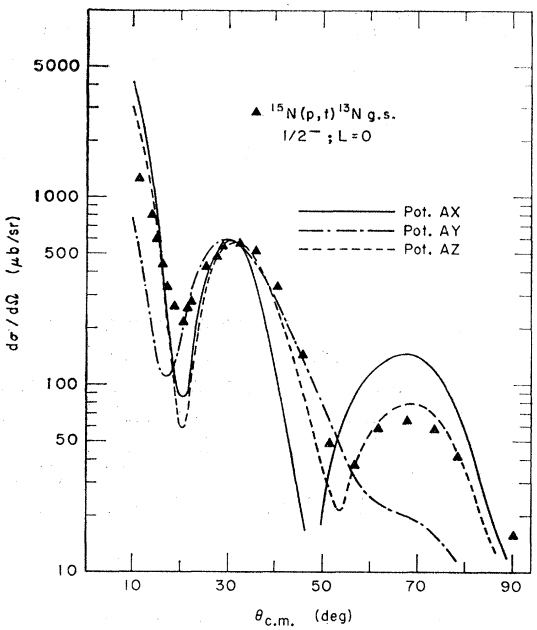

FIG. 15. DWBA fits to the ^{15}N$(p,t)^{13}$N g.s. ($\frac{1}{2}^-$, $L=0$) transition, utilizing the AX, AY, and AZ optical-model potentials given in Table III.

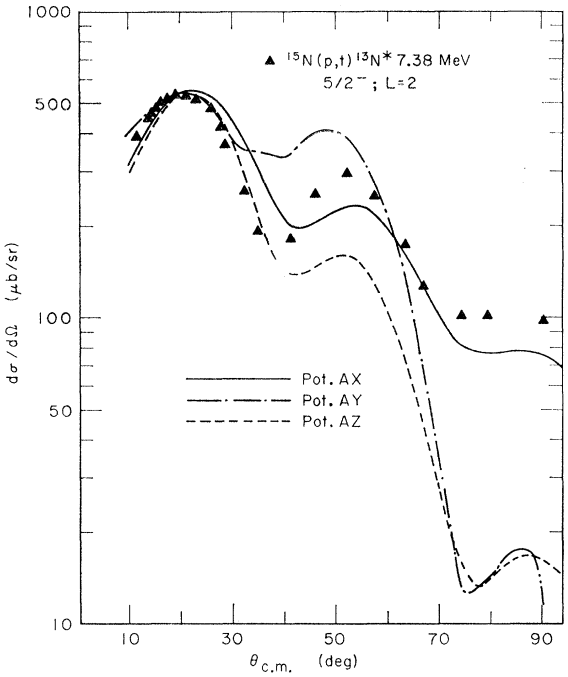

FIG. 16. DWBA fits to the ^{15}N$(p,t)^{13}$N 7.38-MeV ($\frac{5}{2}^-$, $L=2$) transition, utilizing the AX, AY, and AZ optical-model potentials given in Table III.

depth as a linear function of excitation[24,30] were not successful; the DWBA results continued to look better with the AX potential fixed for all excited states.

A. Spectroscopy of Individual Levels

Considerable theoretical interest has been concentrated on nuclei in the $1p$ shell within the framework of the intermediate coupling model. The early calculations of Inglis[31] and Lane[32] were followed by those of Kurath,[33] Boyarkina,[34] and Barker.[35] In all of these calculations the nucleon-nucleon interaction was taken to be purely central and the ratio a/k, where a is the strength of the spin-orbit potential and k is the value of the two-body exchange integral, was left as a variable parameter.

TABLE IV. Intermediate-coupling predictions compared with experimental assignments for the mass-13 levels.

J^π	^{13}N (MeV)	^{13}C (MeV)	Kurath[a] $a/k=5.5$	Boyarkina[b] $a/k=4.2$	Barker[c] $a/k=3.5$	Halbert *et al.*[d]	Cohen and Kurath[e]
$\frac{1}{2}^-$	0.0	0.0	0.0	0.0	0.0	0.0	0.0
$\frac{3}{2}^-$	3.51	3.68	3.7	3.7	3.93	3.5	3.7
$\frac{5}{2}^-$	7.38	7.55	5.3	6.1	7.11	7.0	7.4
$\frac{1}{2}^-$	8.93	8.86	10.7	10.4	9.3	9.0	9.0
$\frac{1}{2}^-$	10.78	11.09	12.5	12.4	11.3	···	13.8
$\frac{3}{2}^-$	11.88	11.80	11.3	11.6	10.2	10.2	10.4
$\frac{7}{2}^-$	···	12.40	12.0	12.3	13.5	···	11.1
$\frac{3}{2}^-[T=\frac{3}{2}]$	15.07	15.11	14.5	14.5	13.2	15.0	14.8
$\frac{3}{2}^-$				15.2			14.0
$\frac{5}{2}^-$				16.4			13.2
$\frac{1}{2}^-$				22.2			17.4

[a] Reference 33. [b] Reference 34. [c] Reference 35. [d] Reference 36. [e] Reference 5.

[30] F. G. Perey, Phys. Rev. **131**, 745 (1963); P. C. Sood, Nucl. Phys. **84**, 106 (1966).
[31] D. R. Inglis, Rev. Mod. Phys. **25**, 390 (1953).
[32] A. M. Lane, Proc. Phys. Soc. (London) **A66**, 977 (1953); **A68**, 197 (1954).
[33] D. Kurath, Phys. Rev. **101**, 216 (1956).
[34] A. N. Boyarkina, Izv. Akad. Nauk SSSR, Ser. Fiz. **28**, 337 (1964) [English transl.: Bull. Acad. Sci. USSR, Phys. Ser. **28**, 255 (1964)].
[35] F. C. Barker, Nucl. Phys. **45**, 467 (1963).

TABLE V. Nuclear-structure factors ($C_{ST}G_{NLSJT}$)[a] for the states in mass 13.[b]

J^π	^{13}N (MeV)	^{13}C (MeV)	^{13}N $NLSJT$	^{13}N $C_{ST}G_{NLSJT}$	^{13}C $NLSJT$	^{13}C $C_{ST}G_{NLSJT}$
					20110	0.151
$\frac{1}{2}^-$	0.0	0.0	20001	0.579	20001	0.284
					12110	−0.462
					20110	0.522
$\frac{3}{2}^-$	3.51	3.68	12021	0.565	12021	0.278
					12110	0.177
					12120	0.380
					12120	−0.562
$\frac{5}{2}^-$	7.38	7.55	12021	1.11	12021	0.546
					12130	0.151
					20110	0.328
$\frac{1}{2}^-$	8.93	8.86	20001	0.0103	20001	0.00506
					12110	0.172
					20110	0.0530
$\frac{1}{2}^-$	10.78	11.09	20001	−0.0972	20001	−0.0481
					12110	−0.185
					20110	0.153
$\frac{3}{2}^-$	11.88	11.80	12021	0.256	12021	0.127
					12110	0.0921
					12120	−0.471
$\frac{7}{2}^-$	...	12.40	...	...	12130	−0.933
$\frac{3}{2}^-$ $[T=\frac{3}{2}]$	15.07	15.11	12021	0.560	12021	0.552

[a] See Ref. 4 for a definition of $C_{ST}G_{NLSJT}$. The values shown in the table do not include the $L=0$, $N=1$ terms since these make little contribution to the cross section.
[b] We are indebted to Dr. Kurath for providing us with the appropriate two-nucleon coefficients of fractional parentage.

More recently Halbert *et al.*[36] reported a calculation similar to those above but using the Hamada-Johnston potential[37] for the nucleon-nucleon interaction, rather than a simple central interaction. An alternative approach is the "effective interaction" treatment of the problem, where the nucleon-nucleon potential is not explicitly defined and the matrix elements of the two-body interaction are left as parameters to be determined by experiment. Calculations of this kind have recently been reported by Cohen and Kurath[5] and Barker.[38] In Table IV, which will be referred to in the following discussion, are shown the predictions of these calculations (Refs. 5, 33–36) for the levels in mass 13, along with the experimental assignments.

As mentioned earlier, the two-nucleon transfer theory[4] requires a separate calculation of the nuclear-structure factors (G_{NLSJT}) which are then used in the DWBA calculation. These factors have been calculated using coefficients of fractional parentage derived from Cohen and Kurath's complete intermediate coupling wave functions[5] and are presented in Table V (multiplied by the spin-isospin coupling factor C_{ST}).[4] Harmonic-oscillator wave functions are assumed for the single-particle states in the nuclear structure calculation and the oscillator parameter ν is taken to be 0.32 F^{-2}, which is the same value that True employed for the $1p$ levels in his shell-model calculation of ^{14}N.[39]

The individual transitions are now discussed.

1. 0 MeV, [^{13}N and ^{13}C], $\frac{1}{2}^-$

Two-nucleon transfer selection rules restrict this transition to a pure $L=0$ transfer for the (p,t) reaction but allow both $L=0$ and $L=2$ for the $(p,^3\text{He})$ reaction. The DWBA fits are shown in Fig. 17 and are arbitrarily normalized—the (p,t) independently of the $(p,^3\text{He})$. The theoretical (p,t) cross section is overpredicted at back angles but otherwise gives a reasonably good account of the data. The $(p,^3\text{He})$ fit, which gives a good representation of the envelope of the angular distribution, does not completely account for the forward angle behavior of the data. A better fit can be obtained through the inclusion of a strongly spin-dependent force, which is later referred to and which enhances the $L=0$ component of this transition.

2. 3.51 MeV [^{13}N] and 3.68 MeV [^{13}C], $\frac{3}{2}^-$

Two-nucleon transfer selection rules now restrict the (p,t) transition to be pure $L=2$ while the $(p,^3\text{He})$ is again a mixture of $L=0$ and $L=2$. The DWBA fits to these data,[40] normalized separately and independently of the ground-state transition, are shown in Fig. 18. The (p,t) transition is well predicted by the theory; the $(p,^3\text{He})$ fit does not completely reproduce the back-angle structure, although it gives a good account of the forward-angle behavior.

[36] E. C. Halbert, Y. E. Kim, and T. T. S. Kuo, Phys. Letters **20**, 657 (1966).
[37] T. Hamada and I. D. Johnston, Nucl. Phys. **34**, 383 (1962).
[38] F. C. Barker, Nucl. Phys. **83**, 418 (1966).
[39] W. M. True, Phys. Rev. **130**, 1530 (1963).

[40] Both of these levels could not be resolved from neighboring $\frac{5}{2}^+$ states at 3.56 MeV in ^{13}N and 3.85 MeV in ^{13}C. However, as is later discussed, a $\frac{5}{2}^+$ transition cannot be directly excited by two-nucleon transfer in the $1p$ shell, so that any contribution of these $(\frac{5}{2}^+)$ levels to the cross sections of the allowed $(\frac{3}{2}^-)$ states is thought to be small.

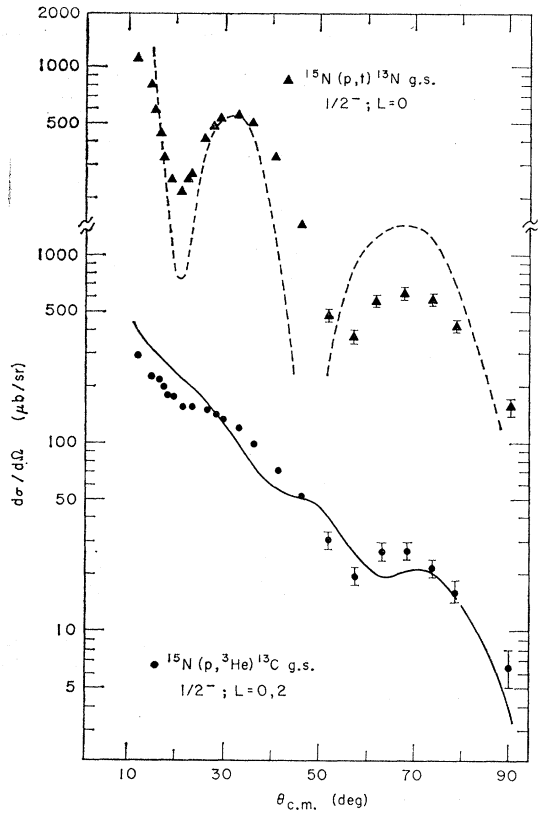

FIG. 17. DWBA fits to the ^{15}N$(p,t)^{13}$N g.s. and ^{15}N$(p,^3\text{He})^{13}$C g.s. transitions.

3. 7.38 MeV [^{13}N] and 7.55 MeV [^{13}C], $\frac{5}{2}^-$

Early ^{12}C+ proton scattering results by Shute *et al.*[41] indicated that the parity of this level (in ^{13}N) should be positive ($\frac{5}{2}^+,\frac{7}{2}^+$), in agreement with the results of other workers.[42] Barker,[43] from an analysis of some ^{12}C$(p,p'\gamma)$ results, agreed that the spin of the level was either $\frac{5}{2}$ or $\frac{7}{2}$, but of negative parity. Based on the results of his intermediate-coupling calculations,[35] which are reproduced in Table IV, Barker assigned this level as $\frac{5}{2}^-$. Similar calculations by both Kurath[33] and Boyarkina[34] predicted a $\frac{5}{2}^-$ level at about 6 MeV of excitation (Table IV); further, Gallman *et al.*[44] show that a value of about 3.5 for a/k, in good agreement with Barker's choice, is required in order to predict a $\frac{5}{2}^-$ level at about 7 MeV of excitation. Nevertheless, recent ^{12}C$(p,p'\gamma)$ experimental results[45] could not clearly distinguish between a $\frac{5}{2}^-$ or a $\frac{7}{2}^-$ assignment.

Transitions to this level are the strongest ones in the ^{15}N$(p,t)^{13}$N spectra. They show a characteristic $L=2$ angular distribution (compare Figs. 13 and 14) which requires either a $\frac{3}{2}^-$ or a $\frac{5}{2}^-$ assignment, and $\frac{3}{2}^-$ seems unlikely in view of the evidence presented above. From this and the relative cross-section results discussed later, we are able to confirm that the level in question is $\frac{5}{2}^-$, a conclusion which has also been reached from recent ^{14}N$(p,d)^{13}$N analyses.[20] The mirror level is observed at 7.55 MeV in ^{13}C via the $(p,^3\text{He})$ reaction. Unlike the ground state and first excited states, however, the $(p,^3\text{He})$ transition is now restricted by angular-momentum coupling to a pure $L=2$ transfer. Consequently, these (p,t) and $(p,^3\text{He})$ $\frac{5}{2}^-$ transitions are expected to have similar angular distributions. The DWBA fits for these transitions are shown in Fig. 19. The theory gives a very good account of the shape of the (p,t) angular distribution and a reasonable fit to the $(p,^3\text{He})$ data, although it has not been able to account for the shift of the first maximum toward smaller angles observed in the $(p,^3\text{He})$ angular distribution. Nevertheless, its angular distribution is well-enough characterized to confirm a $\frac{5}{2}^-$ assignment for the 7.55-MeV level in ^{13}C.

4. 8.93 MeV [^{13}N] and 8.86 [^{13}C], $\frac{1}{2}^-$

This level has been strongly excited in ^{13}N via proton scattering on ^{12}C by a p-wave resonance[41] and a spin-parity of $\frac{1}{2}^-$ has been assigned. It is also strongly excited in the ^{14}N$(^3\text{He},\alpha)^{13}$N reaction (Fig. 6) and the ^{14}N$(p,d)^{13}$N reaction.[20] The analysis of the 8.93-MeV level observed in the ^{15}N$(p,t)^{13}$N reaction (its width is

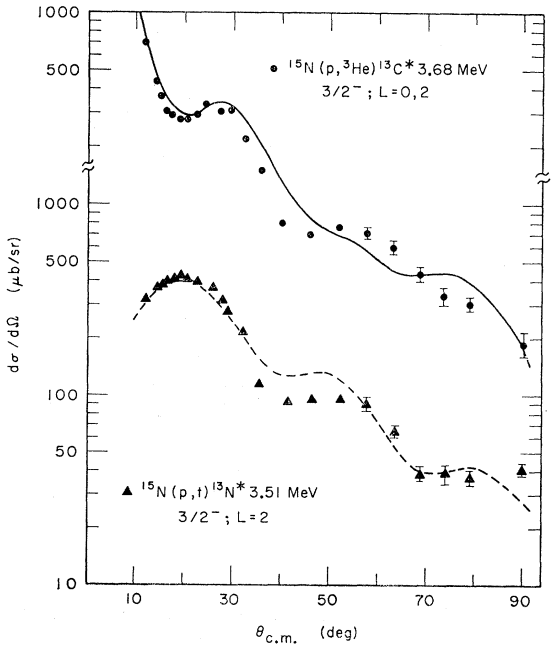

FIG. 18. DWBA fits to the ^{15}N$(p,t)^{13}$N 3.51-MeV and ^{15}N$(p,^3\text{He})^{13}$C 3.68-MeV transitions.

[41] G. G. Shute, D. Robson, V. R. McKenna, and A. T. Berztiss, Nucl. Phys. **37**, 535 (1962).
[42] H. S. Adams, J. D. Fox, N. P. Heydenburg, and G. M. Temmer, Phys. Rev. **124**, 1899 (1961); M. Nomoto, Nucl. Phys. **30**, 514 (1962).
[43] F. C. Barker, Nucl. Phys. **45**, 449 (1963).
[44] A. Gallman, D. E. Alburger, D. H. Wilkinson, and F. Hibou, Phys. Rev. **129**, 1965 (1963).
[45] G. G. Shute and A. M. Baxter, Nucl. Phys. **83**, 460 (1966).

known[18] to be 230 keV) yields a reasonable $L=0$ angular distribution (Fig. 7), in agreement with its $\frac{1}{2}^-$ assignment. A level at 8.86 MeV in ^{13}C, which is probably the mirror of the 8.93-MeV level in ^{13}N, is populated in the ^{15}N$(p,^3$He$)^{13}$C reaction. It has an angular distribution fairly similar to the (p,t) transition, which is understandable on the basis of the nuclear structure calculations; as indicated in Table V, the $L=0$ strength in the $(p,^3$He) cross section is expected to be about a factor of 3 stronger than the $L=2$ strength. As expected, a level at this excitation (8.8 MeV) is also strongly excited in the ^{14}N$(d,^3$He$)^{13}$C reaction (Fig. 6). Intermediate coupling predictions for the appearance of a second $\frac{1}{2}^-$ level in this energy region are generally in very good agreement with experiment (see Table IV).

The DWBA predictions for the angular distributions to these levels are shown in Fig. 20, again normalized independently. These fits are of poor quality compared to the ones previously presented. In addition (see Sec. VB), the relative cross section for this 8.93-MeV $\frac{1}{2}^-$ transition is underpredicted in the DWBA calculation by a factor of 600, whereas agreement to within a factor of 2 is obtained for all the other (p,t) transitions. However, the cross sections predicted from ^{14}N$(^3$He,$\alpha)^{13}$N and ^{14}N$(p,d)^{13}$N DWBA analysis[19,20] for this level agree with experiment to better than a factor of 2. This enormous discrepancy in the (p,t) reaction is difficult to understand and will be discussed later.

5. 9.48 MeV [^{13}N], $\frac{3}{2}^-$ and 9.52 MeV [^{13}C], $(\frac{3}{2}^-)$

This level was originally assigned $\frac{3}{2}^-$ in ^{13}N from proton-scattering results[41] on ^{12}C and until recently was thought to correspond to the second $\frac{3}{2}^-$ level predicted by intermediate coupling theory (Table IV). However, it is virtually absent in the ^{15}N$(p,t)^{13}$N spectra and it is not observed in the ^{14}N$(p,d)^{13}$N or ^{14}N$(^3$He,$\alpha)^{13}$N reactions (Fig. 6).[20,19] The single-nucleon pickup data

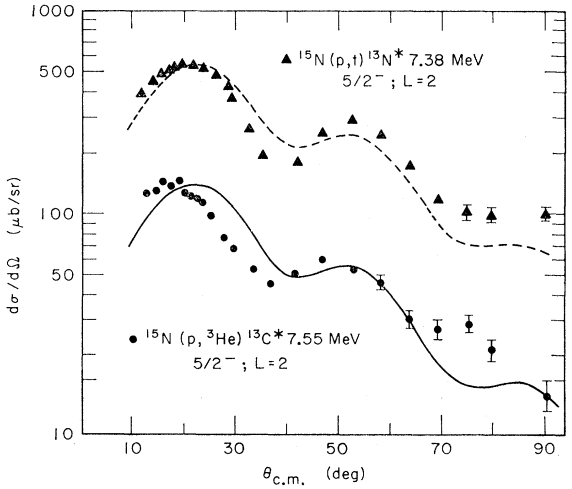

FIG. 19. DWBA fits to the ^{15}N$(p,t)^{13}$N 7.38-MeV and ^{15}N$(p,^3$He$)^{13}$C 7.55-MeV transitions.

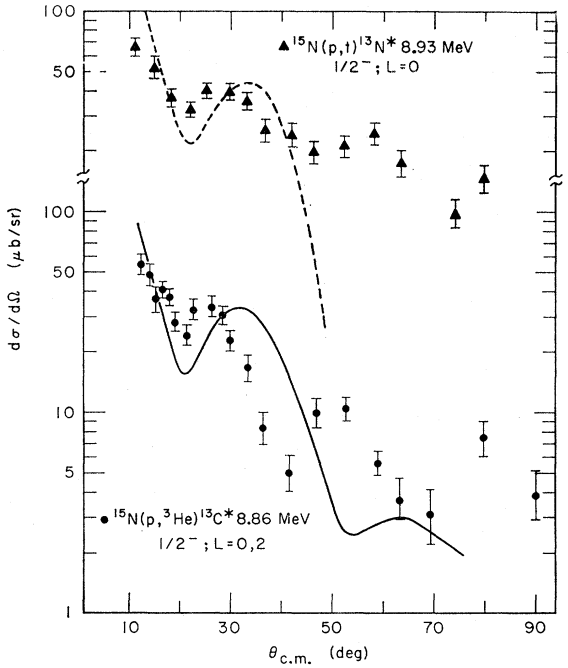

FIG. 20. DWBA fits to the ^{15}N$(p,t)^{13}$N 8.93-MeV and ^{15}N$(p,^3$He$)^{13}$C 8.86-MeV transitions.

are particularly interesting since coefficients of fractional parentage for these reactions[5] show that a second $\frac{3}{2}^-$ level, predicted to lie at about 10 MeV of excitation, should be strongly populated. Furthermore, the structure factors shown in Table V from the Cohen and Kurath work[5] indicate that the second $\frac{3}{2}^-$ level populated in the (p,t) reaction should be roughly only a factor of 5 weaker than the first $\frac{3}{2}^-$ level (3.51 MeV). This would imply a peak angle cross section of about 80 μb and thus should be as strong as the $T=\frac{3}{2}$ level (15.07 MeV, $\frac{3}{2}^-$), which is clearly seen in the spectrum (Fig. 4). The evidence presented here, then, seems to indicate overwhelmingly that the 9.48-MeV $\frac{3}{2}^-$ level in ^{13}N is not primarily composed of a $(1p)^9$ configuration, and is therefore not the second $\frac{3}{2}^-$ level predicted by intermediate coupling theory. This interpretation is supported further by the data of McPherson *et al.*,[46] who studied the beta decay of ^{13}O. The log ft values for this decay (and also for the β decay of the mirror ^{13}B nucleus)[47] are in good agreement with intermediate coupling calculations,[5] except for the transition to the 9.48-MeV $\frac{3}{2}^-$ level in ^{13}N. In fact, it is possible that this particular level contains appreciable $(2s,1d)^2$ admixtures.[5] Such configurations could not be excited in the β decay of ^{13}O and would not be appreciably excited in these nuclear reactions. The second $\frac{3}{2}^-$ level predicted by theory is found to lie at 11.9 MeV, as discussed below.

[46] R. McPherson, R. A. Esterlund, A. M. Poskanzer, and P. L. Reeder, Phys. Rev. **140**, B1513 (1965).

[47] A. Marques, A. J. P. L. Policarpo, and W. R. Phillips, Nucl. Phys. **36**, 45 (1962).

However, a level at 9.52 MeV is excited in the $^{15}N(p,^3He)^{13}C$ reaction, which is relatively strong in comparison to the other levels in this region (Fig. 4 and Table II). A level at this excitation has also been observed in the $^{14}N(d,^3He)^{13}C$ reaction (Fig. 6) which, although weakly populated, is excited stronger than any of the positive-parity levels of ^{13}C. This is a good indication that the 9.52-MeV level in ^{13}C is of negative parity and one might consider it to be the $\frac{3}{2}^-$ mirror of the 9.48-MeV $\frac{3}{2}^-$ level in ^{13}N.[18] The angular distribution seems to be predominantly $L=2$ (compare Figs. 12, 13, and 14), which is consistent with a $\frac{3}{2}^-$ assignment. However, a puzzling aspect about this $(p,^3He)$ transition is its appreciable cross section (Table II), especially relative to the missing mirror (p,t) transition. Both of these levels—the 9.48-MeV in ^{13}N and the 9.52-MeV in ^{13}C—can be expected to mix with neighboring $\frac{3}{2}^-$ levels, the nearest being the 11.90-MeV level, which is discussed below. This last level has strong components of quartet spin states,[34] which would be "S forbidden" in the (p,t) reaction (see Ref. 2). Such components mixed into the 9.5-MeV $\frac{3}{2}^-$ level could favor the $(p,^3He)$ transition.

6. *10.78 MeV* [^{13}N], $\frac{1}{2}^-$, *and 11.09 MeV* [^{13}C], $(\frac{1}{2}^-)$

A new state in the ^{13}N spectrum possessing a small cross section (less than that to the 6.38-MeV $\frac{5}{2}^+$ level) is observed at 10.78 MeV; tritons from this level show an angular distribution sharply peaked forward at small angles (Fig. 7). A level at this excitation is also weakly excited in the $^{14}N(^3He,\alpha)^{13}N$ reaction (Fig. 6) although here it is much more strongly populated than any of the positive-parity levels. The relative strength with which the 10.78-MeV level is populated in the $(^3He,\alpha)$ reaction indicates a level of negative parity and its $L=0$ angular distribution (compare Figs. 13 and 14) in the (p,t) reaction (albeit with very poor statistics) indicates a probable spin and parity of $\frac{1}{2}^-$.

In contrast to the (p,t) data, the $(p,^3He)$ transition to a level at 11.09 MeV in ^{13}C, which is probably the mirror of the one above, is more strongly populated. Although only a few angles were taken, the $^{14}N(d,^3He)^{13}C$ reaction (Fig. 6) excites a level at 11.1 MeV, in good agreement with this value. There are two known[18] levels in this region of ^{13}C, at 11.01 and 11.08 MeV, and it would appear from our energy analysis that the second one is populated in the $^{15}N(p,^3He)^{13}C$ reaction. (The level at 11.01 MeV has been tentatively assigned as $\frac{1}{2}^+$, which one would not expect to be appreciably excited.)

The angular distribution of this $^{15}N(p,^3He)^{13}C$ transition is presented in Fig. 11 and indicates a mixture of $L=0$ and $L=2$ transfers, which would be consistent with either a $\frac{1}{2}^-$ or a $\frac{3}{2}^-$ assignment. The assumption that the 10.78-MeV level in ^{13}N and the 11.09-MeV level in ^{13}C correspond to the third $\frac{1}{2}^-$ state predicted by theory (Table IV) produced the DWBA fits shown in

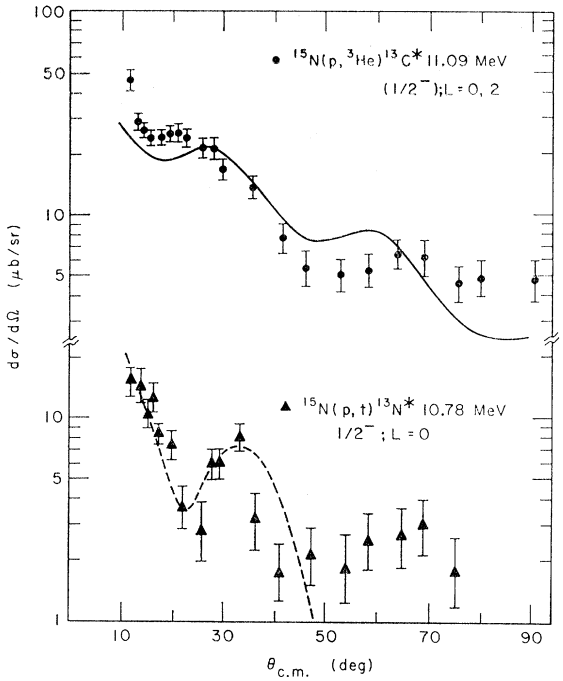

FIG. 21. DWBA fits to the $^{15}N(p,t)^{13}N$ 10.78-MeV and $^{15}N(p,^3He)^{13}C$ 11.09-MeV transitions.

Fig. 21. The $L=0$ shape for the (p,t) transition is well reproduced over the peak and, as we later discuss, the relative cross section of this level is in much better agreement for this choice than with a $\frac{3}{2}^-$ ($L=2$) assignment. The $(p,^3He)$ angular distribution is also reasonably well fit for a level at this high excitation. An assignment of $\frac{1}{2}^-$ is consistent with the above fits and a complete DWBA analysis of the $^{14}N(^3He,\alpha)^{13}N$ data[19] confirms this conclusion.

7. *11.88 MeV* [^{13}N], $\frac{3}{2}^-$, *and 11.80 MeV* [^{13}C], $(\frac{3}{2}^-)$

This level in ^{13}N has been recently observed in single-nucleon transfer reactions[19,20] on ^{14}N (Fig. 5) through a $p_{3/2}$ neutron pickup. An analysis of the intermediate coupling wave functions for the various final states[5] shows that the $\frac{5}{2}^-$, 7.38-MeV level; the $\frac{1}{2}^-$, 8.93-MeV level; and a $\frac{3}{2}^-$ level should all have the same dominant configuration $|(p_{1/2})_1^2,(p_{3/2})^{-1};J\rangle$, and consequently these would all be expected to be strongly excited in single-nucleon transfer reactions on ^{14}N. All three are indeed strongly excited, in good agreement with Cohen and Kurath's spectroscopic factors,[5] and on this basis a $\frac{3}{2}^-$ assignment[20] was made for the level at about 11.9 MeV in ^{13}N. A level at 11.88 MeV has been observed in the $^{15}N(p,t)^{13}N$ reaction and one at 11.80 MeV in the $^{15}N(p,^3He)^{13}C$ reaction—this latter level most likely being the mirror of the one in ^{13}N. This ^{13}C level has also been observed in $^{14}N(d,^3He)^{13}C$ (Fig. 6) and $^{13}C(^3He,^3He')^{13}C$ reactions.[19] The (p,t) reaction populating a $\frac{3}{2}^-$ level is restricted by two-nucleon transfer

selection rules to a pure $L=2$ transfer and the angular distribution of the 11.88-MeV transition is shown in Fig. 8. The $(p,^3\mathrm{He})$ transition, on the other hand, can be populated by both $L=0$ and $L=2$ components and its angular distribution is given in Fig. 11.

The DWBA fits for these levels, using intermediate coupling wave functions for the second predicted $\frac{3}{2}^-$ level, are given in Fig. 22. For the (p,t) transition, both a representative $L=0$ transition at this excitation and an $L=2$ transition are compared with the data. It can be seen that $L=2$ gives a somewhat better over-all fit, which is consistent with the $\frac{3}{2}^-$ assignment. The DWBA calculation is, however, unable to account for the small-angle behavior observed. This shift of the most forward experimental maximum to smaller angles with increasing excitation has been observed in other (p,t) transitions (Figs. 13 and 14). The theory, on the other hand, exhibits a slight shift outward in angle with increasing excitation. The $^{15}\mathrm{N}(p,t)^{13}\mathrm{N}$ 7.38-MeV ($L=2$) transition gave a slight indication of this effect, although not so drastic as observed here. The $(p,^3\mathrm{He})$ fit, on the other hand, is quite good, especially for such a highly excited state. Both the structure and the envelope of the cross section are well predicted by the theory, which gives a good indication for a $\frac{3}{2}^-$ assignment to the 11.80-MeV level in $^{13}\mathrm{C}$.

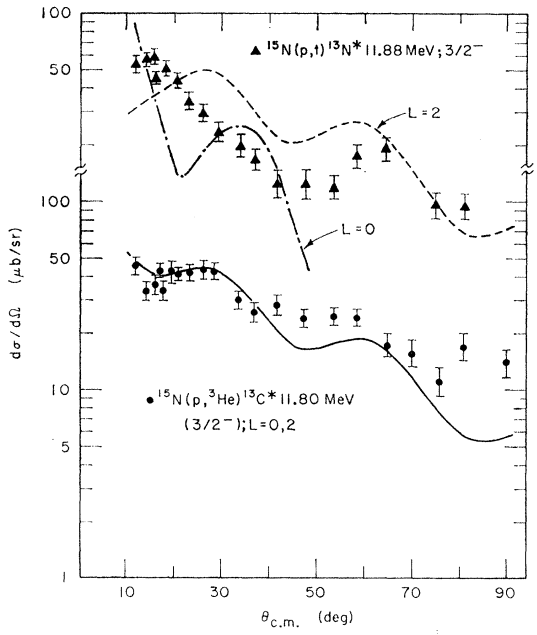

FIG. 22. DWBA fits to the $^{15}\mathrm{N}(p,t)^{13}\mathrm{N}$ 11.88-MeV ($L=2$) and $^{15}\mathrm{N}(p,^3\mathrm{He})^{13}\mathrm{C}$ 11.80-MeV transitions. A representative $L=0$ fit is also shown for the (p,t) reaction.

8. 12.40 MeV [^{13}C], $\frac{7}{2}^-$

A level at 12.40 MeV in $^{13}\mathrm{C}$ was excited fairly strongly in the $^{15}\mathrm{N}(p,^3\mathrm{He})^{13}\mathrm{C}$ reaction, although its counterpart in the $^{15}\mathrm{N}(p,t)^{13}\mathrm{N}$ spectra was completely absent. A previously reported level at 12.44-MeV excitation[18] in $^{13}\mathrm{C}$ has been tentatively assigned as $\frac{1}{2}^-$. This level at 12.40 MeV had a width consistent with the recently reported value of 90 keV,[48] in contrast with other reports on the width of a level at this excitation of about 300 keV.[49] Other levels are also observed in this region in the $^{15}\mathrm{N}(p,^3\mathrm{He})^{13}\mathrm{C}$ reaction at about 12.2 and 12.6 MeV and these could be the cause of the differing widths reported for this state. Although the 12.40-MeV level was not well resolved at most angles from these other peaks, its angular distribution was extracted and is shown in Fig. 12.

The angular distribution for this level has a reasonably pure $L=2$ shape at small angles (compare Figs. 13, 14), which would imply that this was a transition to a $\frac{5}{2}^-$ or $\frac{7}{2}^-$ final state, rather than to a $\frac{1}{2}^-$ state. Intermediate coupling theory (Table IV) would argue for a $\frac{7}{2}^-$ assignment. More importantly, this state is absent in the $^{15}\mathrm{N}(p,t)^{13}\mathrm{N}$ spectra and there is no evidence for a level in this range of excitation in either the $^{14}\mathrm{N}(^3\mathrm{He},\alpha)^{13}\mathrm{N}$ or $^{14}\mathrm{N}(d,^3\mathrm{He})^{13}\mathrm{C}$ reactions (Fig. 6) or in the $^{14}\mathrm{N}(p,d)^{13}\mathrm{N}$ reaction.[20] A $\frac{7}{2}^-$ assignment is the only one consistent with these observations since of the allowed $1p$-shell pickup final states for this $(p,^3\mathrm{He})$ reaction $(\frac{1}{2}^-,\frac{3}{2}^-,\frac{5}{2}^-,\frac{7}{2}^-)$ only the $\frac{7}{2}^-$ state is J (or j) forbidden in all the other reactions. The DWBA fit based on a $\frac{7}{2}^-$ assignment[50] ($L=2$) is shown in Fig. 23. The theory gives a satisfactory account of the data, predicting quite well the envelope of the cross section. For these reasons, then, the assignment of this state as $\frac{7}{2}^-$ rather than the earlier $\frac{1}{2}^-$ seems warranted.

9. 15.07 MeV [^{13}N] and 15.11 MeV [^{13}C], $\frac{3}{2}^-$, $T=\frac{3}{2}$

These two levels populated in the $^{15}\mathrm{N}(p,t)^{13}\mathrm{N}$ and $^{15}\mathrm{N}(p,^3\mathrm{He})^{13}\mathrm{C}$ reactions were reported earlier[51] and will not be discussed in any detail here. The excitations observed are in good agreement with most intermediate coupling calculations (Table VI), except for the results of Barker,[35] which place them almost 2 MeV too low. These are transitions from the same initial to identical final states and as such proceed through a pure ($S=0$, $T=1$) $L=2$ transfer of two nucleons for both transitions. The differential cross sections for both are virtually the same, as shown in Figs. 8 and 12, and are discussed in more detail in Ref. 51; the DWBA fit to the (p,t) transition is given in Fig. 23. [The fit to the $(p,^3\mathrm{He})$ transition was virtually the same as the (p,t)

[48] D. E. Grace and B. D. Sowerby, Nature **206**, 494 (1965).
[49] T. W. Bonner, A. A. Kraus, Jr., J. B. Marion, and J. P. Schiffer, Phys. Rev. **102**, 1348 (1956); J. H. Gibbons and R. H. Macklin, *ibid.* **137**, B1508 (1965).

[50] There is a known (see Ref. 18) $\frac{7}{2}^-$ state at lower excitation—10.36 MeV in $^{13}\mathrm{N}$—which is excited by an f-wave resonance in $^{12}\mathrm{C}+p$ scattering (Ref. 41). As such, it does not appear in an intermediate coupling calculation restricted to the $1p$ shell. This 10.36-MeV ($\frac{7}{2}^-$) level is very weakly excited in the $^{15}\mathrm{N}(p,t)^{13}\mathrm{N}$ reaction and there is no evidence for a level at this excitation in the $(p,^3\mathrm{He})$ spectrum.
[51] J. Cerny, R. H. Pehl, G. Butler, D. G. Fleming, C. Maples, and C. Detraz, Phys. Letters **20**, 35 (1966).

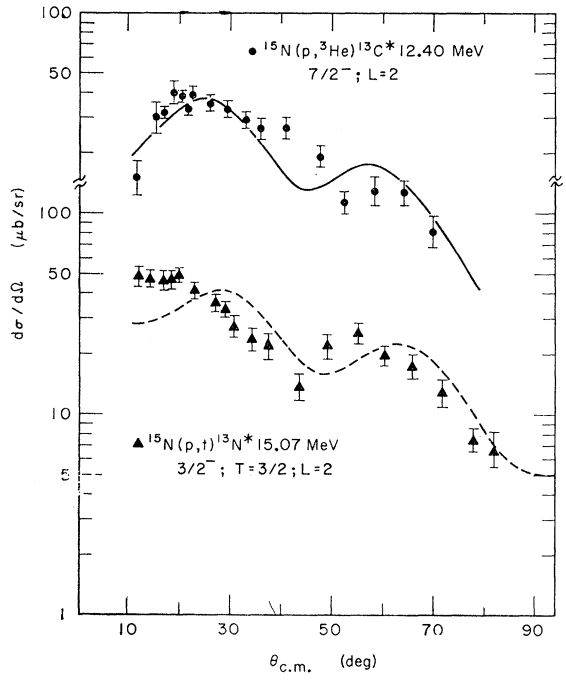

FIG. 23. DWBA fits to the ^{15}N(p,^{3}He)^{13}C 12.40-MeV and ^{15}N(p,t)^{13}N 15.07-MeV ($T=\frac{3}{2}$) transitions.

and is not shown.] The same effect observed earlier in the ^{15}N(p,t)^{13}N 11.88 MeV ($\frac{3}{2}^-$) transition also appears in this (p,t) transition—namely, that the data peak at considerably smaller angles than the theoretical fit. Nevertheless, the DWBA fit does reproduce the observed structure and, considering that this is such a highly excited level, is still reasonable.

10. 6.38 MeV [^{13}N] and 6.87 MeV [^{13}C], $\frac{5}{2}^+$

Insofar as the ground state of ^{15}N can be represented by a $(1p)^{11}$ configuration, then the direct pickup of two nucleons can only excite negative-parity states in the final nucleus. Hence, the population of positive-parity levels must be due to other effects, such as $(2s,1d)^2$ impurities in the ^{15}N ground state or an additional mechanism such as core excitation or knockout. (Compound-nucleus contributions are expected to be negligible at these high bombarding energies.) Only two of the experimentally resolvable positive-parity levels were consistently observed in both the (p,t) and (p,^{3}He) spectra; the first $\frac{1}{2}^+$ level at 2.37 and 3.09 MeV in ^{13}N and ^{13}C, respectively, and the second $\frac{5}{2}^+$ level at 6.38 and 6.87 MeV, respectively. In both spectra, the $\frac{5}{2}^+$ transition is much stronger and angular distributions populating it are shown in Fig. 9. Also of interest in our attempt to interpret the population of these $\frac{5}{2}^+$ states is the ^{13}C(p,t)^{11}C $\frac{7}{2}^-$ transition discussed elsewhere[15,52]; it is J forbidden on the basis of a two-neutron pickup reaction on a pure $(1p)^9$ ^{13}C target, but is populated relatively strongly. Its angular distribution is also shown in Fig. 9. [In the following discussion, a knockout mechanism has been disregarded, in view of the relative population of the $\frac{1}{2}^+$ and $\frac{5}{2}^+$ levels and since this mechanism has been shown to be inadequate in a treatment of "j-forbidden" (d,p) reactions,[53] where its influence might even be greater than in the (p,t) reaction.]

Although the shape of the ^{13}N($\frac{5}{2}^+$) angular distribution is not that normally observed for an $L=3$ transfer,[54] as would be required for pickup from a $(1d)^2$ impurity in the ^{15}N ground state, it is possible to obtain a reasonable fit to these data. In Fig. 24 are shown DWBA fits for this transition as well as for the ^{13}C-(p,t)^{11}C ($\frac{7}{2}^-$) transition reported previously.[15,52] Two curves are shown for each transition, corresponding to different choices for the oscillator parameter of the bound-state wave function: $\nu=0.32$ and 0.40 for the $\frac{5}{2}^+$ transition and $\nu=0.32$, 0.46 for the $\frac{7}{2}^-$ transition. The larger values correspond to different radii for matching the Hankel-function tail at the nuclear surface. (This procedure is discussed in more detail later.) Since it is not clear how to treat the bound-state wave function for a $(1d1p)$ $L=3$ or a $(1p1f)$ $L=4$ transition (a problem which also arises in the analysis of single-nucleon transfer reactions[55]), these larger values of ν are perhaps not unreasonable and their use does result in improved fits to the data.

Under these assumptions and using the configurations predicted from weak-coupling calculations[56] for this ^{13}N ($\frac{5}{2}^+$) state, a $(15\pm5)\%$ admixture of $(1d_{5/2})^2$ in the ^{15}N ground state would be necessary to account for the relative strength of the observed transition. The relative population of the 6.38-MeV $\frac{5}{2}^+$ and 2.37-MeV $\frac{1}{2}^+$ levels in ^{13}N can be understood through a larger amount of $(d_{5/2})^2$ than of $(s_{1/2})^2$ in the ^{15}N ground state—a conclusion consistent with an analysis of the negative-parity states populated in the ^{15}N(^{3}He,α)^{14}N reaction.[57] Similar results for ^{16}O have been obtained based on the population of its 5.28-MeV $\frac{5}{2}^+$ level in the ^{16}O(d,^{3}He)^{15}N reaction.[28]

However, the relative population of the $\frac{1}{2}^+$ and $\frac{5}{2}^+$ levels of ^{13}N can also be understood on the basis of a core-excitation pickup reaction[58] proceeding through the

[52] D. G. Fleming, J. Cerny, and N. K. Glendenning, Phys. Rev. **165**, 1153 (1968).

[53] G. Strobel, Phys. Rev. **154**, 941 (1967).

[54] J. Cerny, D. G. Fleming, and C. C. Maples (unpublished); J. R. Maxwell, G. M. Reynolds, and N. M. Hintz, University of Minnesota Annual Progress Report, 1965, p. 98 (unpublished).

[55] N. Austern, Phys. Rev. **136**, B1743 (1964); R. Sherr, B. F. Bayman, E. Rost, M. E. Rickey, and C. G. Hoot, *ibid.* **139**, B1272 (1965); C. Glashausser, M. Kondo, M. E. Rickey, and E. Rost, Phys. Letters **14**, 113 (1965).

[56] F. C. Barker, Nucl. Phys. **28**, 96 (1961); T. Sebe, Progr. Theoret. Phys. (Kyoto) **30**, 290 (1963).

[57] G. C. Ball and J. Cerny, Phys. Letters **21**, 551 (1966); G. C. Ball (private communication).

[58] S. K. Penny and G. R. Satchler, Nucl. Phys. **53**, 145 (1964); B. Kozlowsky and A. de-Shalit, *ibid.* **77**, 215 (1966); S. K. Penny, Ph.D. thesis, University of Tennessee, 1966 (unpublished); F. S. Levin, Phys. Rev. **147**, 715 (1966).

^{15}N 5.28-MeV level.[15] Further, the observed angular distribution to the ^{13}N ($\frac{5}{2}^+$) state [and the ^{11}C ($\frac{7}{2}^-$) state] is presumably also consistent with such a mechanism. Clearly, much more theoretical work and more extensive data are required to establish the mechanism involved in populating these positive-parity states.

B. Comparison of Relative Cross Sections

The discussion of relative cross sections is concentrated on the ^{15}N$(p,t)^{13}$N reaction, since a previous report[52] has shown that interference terms in the $(p,^3\text{He})$ reaction are liable to drastically affect its cross section. Before discussing the theoretical cross sections, it is well to review how the form factor is treated in the calculation. Since the bound-state wave function is represented by a harmonic oscillator, it is matched at the nuclear surface to a Hankel-function tail. For a pickup reaction, the increasing separation energy of the pair with excitation has a damping effect on the magnitude of the Hankel function and this results in an increase in the matching radius with increasing excitation. For a given L transfer, this tends to cause an increase in the predicted two-nucleon cross section with excitation, although the magnitude of this increase can be quite sensitive to the chosen optical-model potential, as will be indicated later. An alternative method is to match the Hankel-function tail at the same radius for all excited states, which necessitates a slight increase in the oscillator parameter ν with excitation. Both approaches have been tried and noticeably better results are obtained with the latter.

Relative cross sections for these two calculations are compared with experiment in Table VI for two choices of the optical-model potential, AX and AZ (Table III), and using the nuclear structure factors shown in Table V. Both calculations have been arbitrarily adjusted to give the best agreement with experiment. The calculation in which the oscillator parameter is fixed at $\nu=0.32$ and the matching radius is correspondingly increased gives noticeably poorer results for relative cross sections than the procedure adopted whereby the matching radius is fixed (at the ground-state value of 3.60 F) and the oscillator parameter adjusted. The variation in agreement of the experimental and theoretical relative cross sections is indicated by the quantity B in Table VI, which was calculated by minimizing the average value of the larger ratio of experiment and theory for all the indicated levels and then subtracting one from the result ($B=0$ for perfect agreement). B varies from a value of 1.53 (AX potential with constant ν) to a value of 0.31 (AZ potential with

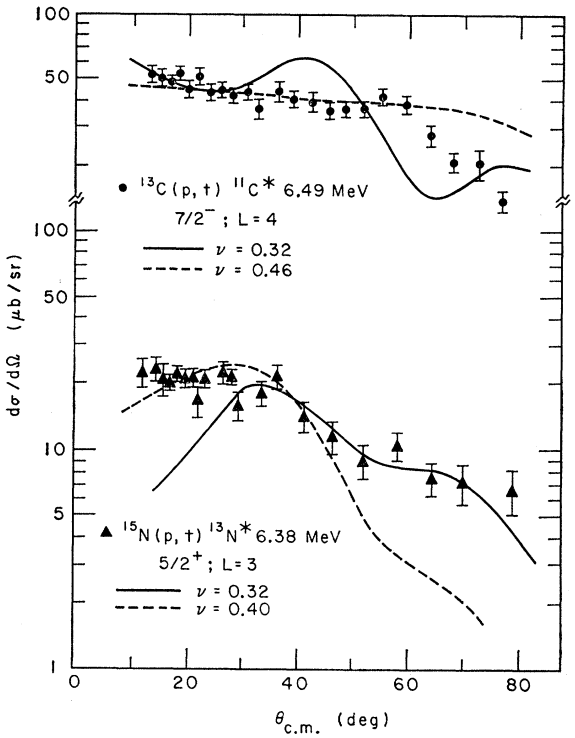

FIG. 24. DWBA fits to the ^{13}C$(p,t)^{11}$C 6.49-MeV and ^{15}N$(p,t)^{13}$N 6.38-MeV transitions, utilizing different choices for the oscillator parameter ν in the bound-state wave function.

TABLE VI. ^{15}N$(p,t)^{13}$N relative cross sections for different form factors and optical-model potentials.

J^π	Exc. (MeV)	$\sigma_T(\mu b)$ (expt.) (10°–90°, c.m.)	Relative σ_T (expt.)	Matching R(F)	AX σ_T (rel.)	AZ σ_T (rel.)	ν	AX σ_T (rel.)	AZ σ_T (rel.)
$\frac{1}{2}^-$	0.0	941	1.00	3.58	0.200[a]	0.500	0.318	0.400[a]	0.790
$\frac{3}{2}^-$	3.51	652	0.693	3.70	0.444	0.510	0.334	0.676	0.616
$\frac{5}{2}^-$	7.38	1271	1.35	3.82	2.06	1.92	0.348	2.22	1.73
$\frac{1}{2}^-$	8.93	130	0.138	[3.84	0.00024	0.00025][b]	[0.351	0.00021	0.00022][b]
$\frac{1}{2}^-$	10.78	17.6	0.0187	3.89	0.0266	0.0244	0.357	0.0184	0.0188
							[0.357	0.0968	0.0675][b]
$\frac{3}{2}^-$	11.88	93	0.0988	3.94	0.120	0.0900	0.362	0.0855	0.0576
$\frac{3}{2}^-[T=\frac{3}{2}]$	15.07	115	0.122	4.03	0.544	0.359	0.372	0.263	0.181
					$B=1.53$	0.68		0.59	0.31

[a] The ground state is expected to show poor agreement for the AX potential since this potential produced a relatively poor fit to the data (Fig. 15).
[b] Not included in the calculation of B.

constant $R=3.60F$ and a 17% variation in ν). For both calculations, the theoretical results using optical potential AZ are in much better agreement with experiment than those using potential AX. Other choices were tried (including AY of Table III) and in no case was there a significantly greater difference than between AX and AZ. It is disappointing that potential AX shows the worst agreement in reproducing the relative cross sections, since it gives better over-all fits to the data and is the potential used in the previous discussion. However, potential AZ shows the best fit to the ground-state transition (Fig. 15) and also gives a reasonable fit to all the excited states (an example is shown in Fig. 16).

The data in Table VI represent the first time, to our knowledge, that comparisons of relative cross sections in two-nucleon transfer reactions over 15 MeV of excitation have been made. The calculation involving a fixed matching radius for the final states must be considered as being in quite good agreement with experiment (and is used hereafter) and insofar as our adjustment of the oscillator parameter ν would not markedly affect the amplitudes of the intermediate coupling wave functions of Cohen and Kurath,[5] then these wave functions must be regarded as giving a good description of the final states populated in the ^{15}N-$(p,t)^{13}$N reaction.

Two points of interest appear in Table VI. First, it is important to note that the cross section to the very weakly excited 10.78-MeV level in ^{13}N, which we earlier assigned as $\frac{1}{2}^-$, is in good agreement with calculation. In fact, assuming this level to be the next $\frac{3}{2}^-$ state gives a theoretical value for the cross section (shown in brackets in Table VI) which, on the average, is a factor of 4 too large. Second, of equal interest is the transition to the 8.93-MeV $\frac{1}{2}^-$ state, for which the relative cross section is predicted to be a factor of 600 too low. However, one should note that good agreement is obtained in the ^{14}N$(p,d)^{13}$N and ^{14}N$(^3$He$,\alpha)^{13}$N calculations[20,19] for this level. We do not understand this large discrepancy; it can perhaps be explained through coherent admixtures of other configurations or by a very complex reaction mechanism.

Table VII presents the relative integrated cross sections for the ^{15}N$(p,^3$He$)^{13}$C reaction and DWBA comparisons similar to those of Table VI. The matching radius for the 3.68-MeV $(\frac{3}{2}^-)$ transition was held constant and the theoretical cross sections are again arbitrarily adjusted to give the best agreement with experiment. Two values of B are shown in the table, B_1 and B_2. The B_1 value arises from all the levels shown in Table VII while B_2 is calculated only for the mirror transitions corresponding to those in Table VI.

In an earlier paper[52] it was reported that the ratios of (p,t) to $(p,^3$He) cross sections for mirror transitions were significantly improved with the introduction of a strong spin dependence in the nucleon-nucleon interaction between the incident proton and the picked-up nucleons. Since this can only affect the $(p,^3$He) relative cross sections, calculations for both a spin-independent, $A^S=A^T$, and the strongly spin-dependent interaction of Ref. 52, $A^S=0.3A^T$, are presented in Table VII. There appears to be little difference between the spin-independent and the spin-dependent results for the B_1 calculation but the B_2 calculation shows a definite preference for the spin-independent interaction for such *relative*-cross-section comparisons. However, the earlier discussion[52] of cross-section ratios has shown that a spin dependence is to be preferred, although it could not account for all the data, and one of the further suggestions made was that a coherent sum on the (LS) quantum numbers of the transferred pair in the $(p,^3$He) reaction should be taken into account. Since the calculations described above have not included this coherence, we would expect that the agreement in relative cross sections for these transitions should be significantly worse than for the mirror (p,t) transitions discussed earlier (Table VI). Comparing the two over

TABLE VII. ^{15}N$(p,^3$He$)^{13}$C relative cross sections for different spin-dependent interactions and optical-model potentials.

				$A^S=A^T$		$A^S=0.3A^T$		
J^π	Exc. (MeV)	$\sigma_T(\mu$b) (expt.) (10°–90°, c.m.)	Relative σ_T (expt.)	AX σ_T (rel.)	AZ σ_T (rel.)	AX σ_T (rel.)	AZ σ_T (rel.)	ν
$\frac{1}{2}^-$	0.0	308	1.00	0.650	1.00	0.612	0.997	0.308
$\frac{3}{2}^-$	3.68	573	1.86	1.04	1.44	1.04	1.28	0.323
$\frac{5}{2}^-$	7.55	270	0.878	1.41	1.26	2.00	1.66	0.337
$\frac{1}{2}^-$	8.86	61	0.198	0.271	0.329	0.198	0.226	0.342
$(\frac{1}{2}^-)$	11.09	52	0.169	0.0690	0.0588	0.0571	0.0479	0.350
$(\frac{3}{2}^-)$	11.80	137	0.445	0.444	0.364	0.361	0.276	0.352
$\frac{7}{2}^-$	12.40	100	0.325	1.31	1.02	0.954	0.693	0.354
$\frac{3}{2}^-[T=\frac{3}{2}]$	15.11	115[a]	0.358	0.319	0.246	0.699	0.395	0.363
				B_1 =0.863	0.760	0.972	0.733	
				B_2[b]=0.498	0.426	0.899	0.710	

[a] This cross section assumed identical to the (p,t) $[T=\frac{3}{2}]$ cross section due to the lack of large-angle data.
[b] This calculation does not include the 8.86-MeV $(\frac{1}{2}^-)$ and 12.40-MeV $(\frac{7}{2}^-)$ levels.

the same range of excitation and for the same optical potential, however, the (p,t) cross sections are found to be only in marginally better agreement with experiment. The agreement in these $(p,^3\mathrm{He})$ cross sections is certainly acceptable—the present theory predicting fairly well those states which are strongly or weakly excited.

It would appear from the above results that a comparison of experimental *relative* cross sections with theory in a $(p,^3\mathrm{He})$ [or $(^3\mathrm{He},p)$] reaction on a $T=\frac{1}{2}$ target does not clarify the discussion presented earlier[52] which indicated (1) a necessity for some spin-dependent nucleon-nucleon interaction in the two-nucleon transfer theory, and (2) the probable necessity for including spin-orbit coupling in the optical potential. DWBA calculations that reliably predicted *absolute* cross sections for these two-nucleon transfer reactions and could incorporate these effects would certainly resolve the problem. Insofar as the first effect is considered, a comparison of experimental and theoretical relative cross sections for $(p,^3\mathrm{He})$ [or $(^3\mathrm{He},p)$] transitions on $T=0$ targets would be expected to be much more sensitive to the presence of a spin-dependent nucleon-nucleon force, since here the neutron-proton pair is transferred in unique ^3S, $T=0$ or ^1S, $T=1$ states. Calculations by Hardy and Towner[59] of the states populated both in the $^{12}\mathrm{C}(^3\mathrm{He},p)^{14}\mathrm{N}$ reaction at 20 MeV[8] and the $^{16}\mathrm{O}(p,^3\mathrm{He})^{14}\mathrm{N}$ reaction at 40 MeV[60] show that a spin dependence, consistent with that used in theoretical calculation and compatible with that used previously by us,[52] is required in order to account for the experimental cross sections. We will further discuss the necessity for including a spin dependence in the two-nucleon DWBA calculation in a forthcoming report on the $^{16}\mathrm{O}(p,^3\mathrm{He})^{14}\mathrm{N}$ and $^{16}\mathrm{O}(p,t)^{14}\mathrm{O}$ reactions.

ACKNOWLEDGMENT

We would like to thank Dr. Dieter Kurath for several valuable communications.

[59] J. C. Hardy and I. S. Towner, Phys. Letters **25B**, 98 (1967).
[60] R. E. Brown, N. M. Hintz, C. G. Hoot, J. R. Maxwell, and A. Scott, University of Minnesota Annual Progress Report, 1966, p. 70 (unpublished).

PHYSICAL REVIEW VOLUME 166, NUMBER 4 20 FEBRUARY 1968

Pology and (d,p) Reactions

W. K. BERTRAM AND L. J. TASSIE
Department of Theoretical Physics, Faculty of Science, Australian National University, Canberra, Australia
(Received 22 September 1967)

Cross sections for (d,p) reactions calculated in the physical region are extrapolated to the Butler pole in order to investigate the possibility of extracting reduced widths. The cross sections are calculated by distorted-wave Born approximation (DWBA), using a method of evaluation yielding cross sections with the correct analytic behavior near the pole. The cross sections in the unphysical region between the pole and the start of the physical region are calculated and compared with the extrapolation of cross sections from the physical region. Detailed calculations are made for two reactions in which the neutron is captured into an s state: $\mathrm{Si}^{28}(d,p)\mathrm{Si}^{29}$ to the ground state, and $\mathrm{C}^{12}(d,p)\mathrm{C}^{13}$ (3.09 MeV). It is found that an effect of the Coulomb interaction prevents accurate extrapolation to the pole for heavy nuclei or low energies. The method of evaluating the DWBA cross section has an advantage over the usual method in that fewer partial waves need be summed.

I. INTRODUCTION

THE amplitude for the stripping reaction $A+d\rightarrow B+p$ for fixed deuteron energy E_d is a function of the variable

$$Q^2=[\mathbf{k}_d-(m_A/m_B)\mathbf{k}_p]^2, \tag{1.1}$$

with a pole,[1,2] the Butler pole, at $Q^2=-\kappa_n^2$. $\mathbf{k}_d$ and $\mathbf{k}_p$ are the deuteron and proton momenta in the c.m. system, and

$$\kappa_n^2=-2m_{nA}B/\hbar^2, \tag{1.2}$$

where B is the binding energy of the captured neutron.

[1] R. D. Amado, Phys. Rev. Letters **2**, 399 (1959).
[2] H. J. Schnitzer, Rev. Mod. Phys. **37**, 666 (1965).

The notation

$$m_{xy}=m_xm_y/(m_x+m_y)$$

is used for reduced masses. The residue at the Butler pole is proportional to the reduced width for the reaction $A+n\rightarrow B$. Amado[1] pointed out the possibility of obtaining this reduced width by extrapolating the stripping cross section to the pole.

Very accurate experimental results are required for this extrapolation, and the reliability of the reduced widths obtained cannot be checked. It thus seems desirable to perform the extrapolation when the reduced width is already known in order to check the reliability of the extrapolation. A way of doing this is by means of